

**Design, Synthesis, and Biological Evaluation of
Pyrimido[4,5-*d*]pyrimidine-2,4(1*H*,3*H*)-diones as Potent
and Selective Epidermal Growth Factor Receptor (EGFR)
Inhibitors against L858R/T790M Resistance Mutation**

Yongjia Hao, Jiankun Lyu, Rong Qu, Yi Tong, Deheng Sun, Fang Feng, Linjiang Tong,
Tingyuan Yang, Zhenjiang Zhao, Lili Zhu, Jian Ding, Yufang Xu, Hua Xie, and Honglin Li

J. Med. Chem., **Just Accepted Manuscript** • DOI: 10.1021/acs.jmedchem.8b00346 • Publication Date (Web): 15 Jun 2018

Downloaded from <http://pubs.acs.org> on June 16, 2018

Just Accepted

“Just Accepted” manuscripts have been peer-reviewed and accepted for publication. They are posted online prior to technical editing, formatting for publication and author proofing. The American Chemical Society provides “Just Accepted” as a service to the research community to expedite the dissemination of scientific material as soon as possible after acceptance. “Just Accepted” manuscripts appear in full in PDF format accompanied by an HTML abstract. “Just Accepted” manuscripts have been fully peer reviewed, but should not be considered the official version of record. They are citable by the Digital Object Identifier (DOI®). “Just Accepted” is an optional service offered to authors. Therefore, the “Just Accepted” Web site may not include all articles that will be published in the journal. After a manuscript is technically edited and formatted, it will be removed from the “Just Accepted” Web site and published as an ASAP article. Note that technical editing may introduce minor changes to the manuscript text and/or graphics which could affect content, and all legal disclaimers and ethical guidelines that apply to the journal pertain. ACS cannot be held responsible for errors or consequences arising from the use of information contained in these “Just Accepted” manuscripts.

1
2
3
4
5
6 **Design, Synthesis, and Biological Evaluation of Pyrimido[4,5-*d*]pyrimidine-**
7 **2,4(1*H*,3*H*)-diones as Potent and Selective Epidermal Growth Factor Receptor**
8 **(EGFR) Inhibitors against L858R/T790M Resistance Mutation**
9
10
11
12
13
14

15 Yongjia Hao^{1,2,‡}, Jiankun Lyu^{1,‡}, Rong Qu^{3,‡}, Yi Tong¹, Deheng Sun¹, Fang Feng³, Linjiang
16 Tong³, Tingyuan Yang¹, Zhenjiang Zhao¹, Lili Zhu¹, Jian Ding³, Yufang Xu^{1,*}, Hua Xie^{3,*},
17
18
19
20 Honglin Li^{1,*}
21
22

23
24 1 Shanghai Key Laboratory of New Drug Design, State Key Laboratory of Bioreactor
25 Engineering, School of Pharmacy, East China University of Science and Technology, Shanghai
26 200237, China.
27
28
29

30
31 2 School of Pharmacy, Guizhou University of Chinese Medicine, Guiyang 550025, China.
32
33

34
35 3 Division of Anti-tumor Pharmacology, State Key Laboratory of Drug Research, Shanghai
36 Institute of Materia Medica, Chinese Academy of Sciences, Shanghai 201203, China.
37
38
39

40 ‡ Authors contributed equally to this work
41
42

43 * To whom correspondence should be addressed. Email: yfxu@ecust.edu.cn, hxie@jding.dhs.org,
44
45 hlli@ecust.edu.cn
46
47
48
49
50
51
52
53
54
55
56
57
58
59
60

ABSTRACT

1
2
3
4
5
6 First-generation epidermal growth factor receptor (EGFR) inhibitors, gefitinib and erlotinib have
7
8 achieved initially marked clinical efficacy for non-small cell lung cancer (NSCLC) patients with
9
10 EGFR activating mutations. However, their clinical benefit was limited by the emergence of
11
12 acquired resistance mutations. In most cases (approximately 60%), the resistance was caused by
13
14 the secondary EGFR T790M gatekeeper mutation. Thus, it is still desirable to develop novel
15
16 third-generation EGFR inhibitors to overcome T790M mutation while sparing wild-type (WT)
17
18 EGFR. Herein, a series of pyrimido[4,5-*d*]pyrimidine-2,4(1*H*,3*H*)-dione derivatives were
19
20 designed and synthesized. Among which, the most potent compound **20g** not only demonstrated
21
22 significant inhibitory activity and selectivity for EGFR^{L858R/T790M} and H1975 cells *in vitro*, but
23
24 also displayed outstanding antitumor efficiency in H1975 xenograft mouse model. The
25
26 encouraging mutant-selective results at both *in vitro* and *in vivo* levels suggested that **20g** might
27
28 be used as a promising lead compound for further structural optimization as potent and selective
29
30 EGFR^{L858R/T790M} inhibitors.
31
32
33
34
35
36
37
38
39
40
41
42
43
44
45
46
47
48
49
50
51
52
53
54
55
56
57
58
59
60

INTRODUCTION

Lung cancer, especially non-small cell lung cancer (NSCLC) is one of the most prevalent malignant tumors, and also a major health problem worldwide, whose five-year survival rate is less than 15% after diagnosis.¹ It is well-known that the epidermal growth factor receptor (EGFR, also known as ErbB1, HER1)-mediated signaling pathways are essential for various biological processes and cancers development and progression, such as cell proliferation, adhesion, migration, differentiation and survival.²⁻⁴ Thus, the EGFR tyrosine kinase has been proven to be an attractive and clinically validated drug target in cancer therapy, in particular for NSCLC treatment. First-generation reversible and quinazoline-based EGFR tyrosine kinase inhibitors (TKIs), including gefitinib (**1**) and erlotinib (**2**), have received approval from US Food and Drug Administration (FDA) for the treatment of NSCLC in 2003 and 2004, respectively (Figure 1).^{5,6} Despite the clinical efficacy of the two drugs have been well established for NSCLC patients with the most common EGFR activating mutations, such as L858R (activating mutation in exon 21) and del E746–A750 (deletions in exon 19).⁷⁻⁹ Unfortunately, a secondary T790M point mutation (the substitution threonine790 with methionine residue) at the gatekeeper position of EGFR has caused approximately 60% NSCLC patients who initially responded to the treatment of first-generation EGFR inhibitors to develop acquired resistance after a median of 10–14 months.¹⁰ Occurrence of the T790M acquired resistance mutation not only seriously affected the improvement of survival rates, but also impaired the quality of life of NSCLC patients.

In order to prevent the acquired resistance caused by the T790M mutation, several second-generation irreversible EGFR inhibitors have been developed.¹¹⁻¹⁴ Afatinib (**3**) is a typical example, which has been approved by FDA as a new first-line treatment for late stage

1
2
3 (metastatic) NSCLC patients with EGFR exon 19 deletions or exon 21 L858R substitution
4 mutations in 2013 (Figure 1).¹⁵ Although afatinib was highly active *in vivo* in xenograft models
5 driven by EGFR^{L858R/T790M}, it didn't increase objective response rate in clinical trial of NSCLC
6 patients who have been developed resistance to gefitinib or erlotinib on account of the narrow
7 therapeutic window towards wild-type (WT) EGFR.¹⁶ Therefore, there is still an unmet clinical
8 need to develop third-generation EGFR TKIs, namely, mutant-selective EGFR-TKIs. These
9 inhibitors have potent selectivity for EGFR T790M while sparing wild-type EGFR, so can
10 improve the efficacy and reduce the toxicity associated with the inhibition of WT EGFR protein.
11 WZ4002 (**4**)¹⁷ with an anilinepyrimidine core was the first such type of mutant-selective EGFR-
12 TKIs, nevertheless, which did not progress into clinical development. Simultaneously, another
13 two mutant-selective small molecule EGFR inhibitors have been publicly reported, that are CO-
14 1686 (**5**, Rociletinib)^{18,19} and AZD9291 (**6**, Osimertinib)^{20,21}. These two agents demonstrated
15 good potency and prominent selectivity for EGFR L858R/T790M over WT EGFR (Figure 1).
16 Furthermore, according to its significant clinical benefits, FDA has accelerated approved
17 compound **6** to treat advanced NSCLC patients with EGFR^{T790M} acquired resistance mutation,
18 who have progressed on or after prior treatment with other EGFR-targeted therapy.²²
19
20
21
22
23
24
25
26
27
28
29
30
31
32
33
34
35
36
37
38
39
40

41 **Figure 1**

42
43
44
45
46
47 Recently, we reported a study of developing a series of mutant-selective EGFR inhibitors with
48 a C4-alkyl-1,4-dihydro-2*H*-pyrimido[4,5-*d*][1,3]oxazin-2-ones scaffold.²³ By a 3D-comformer
49 based scaffold hopping strategy, we designed a new scaffold of pyrimido[4,5-*d*]pyrimidine-
50 2,4(1*H*,3*H*)-dione as a starting point to develop a series of novel EGFR^{L858R/T790M} selective
51
52
53
54
55
56
57
58
59
60

1
2
3 inhibitors. At the end of a 3-round structural optimization, our candidate compound **20g** displays
4 a favorable selectivity against double-mutant EGFR at both enzymatic and cellular levels.
5
6 Compound **20g** also shows a good selectivity profile in *in vivo* study. Our study provides a new
7
8 scaffold of mutant-selective EGFR inhibitors by an efficient *in-silico* scheme.
9
10
11
12

13 **Figure 2**

14
15
16
17
18

19 **CHEMISTRY**

20
21

22 As shown in Scheme 1, compounds **14a-e** were synthesized starting from 1,3-benzendiamine,
23 followed by treatment with di-*tert*-butyl dicarbonate to give Boc-protected amine (**8**). Then,
24 compound (**8**) was reacted with ethyl 2,4-dichloropyrimidine-5-carboxylate to yield ethyl 4-((3-
25 ((*tert*-butoxycarbonyl)amino)phenyl)amino)-2-chloropyrimidine-5-carboxylate (**9**) in a good
26
27 yield. Hydrolysis of the carboxylic ethyl ester group by 1 M NaOH to afford carboxylic acid
28
29 (**10**), and the key intermediates (**11**) were generated with arylamines by replacement of the
30
31 chloride in the pyrimidine. The amide derivatives (**12**) were prepared from condensation
32
33 carboxylic acid derivatives (**11**) with methylamine hydrochloride. Direct cyclization with 1,1'-
34
35 carbonyldiimidazole to obtain the ring-closure intermediates (**13**). Finally, **13** were deprotected
36
37 with trifluoroacetic acid in dichloromethane and reacted with acryloyl chloride to produce the
38
39 target compounds **14a-e**.
40
41
42
43
44
45
46
47
48

49 **Scheme 1**

50
51
52
53
54
55
56
57
58
59
60

1
2
3 To compare the influence of activity, we synthesized a series of final compounds with
4 different substituted alkyl groups at 3-position of pyrimido[4,5-*d*]pyrimidine-2,4(1*H*,3*H*)-dione
5 moiety (Scheme 2). Commercially available 2,4-dichloro-5-pyrimidinecarbonyl chloride was
6
7
8 reacted with ammonium hydroxide to give 2,4-dichloropyrimidine-5-carboxamide (**15**).
9
10 Intermediates (**17**) were generated with Boc-protected amine and appropriate arylamines by
11 replacement of the chloride at 4, 2-position of pyrimidine, respectively. Then, the ring-closure
12
13
14
15
16
17
18
19
20
21
22
23
24
25
26
27
28
29
30
31
32
33
34
35
36
37
38
39
40
41
42
43
44
45
46
47
48
49
50
51
52
53
54
55
56
57
58
59
60

compounds (**18**) were obtained based on the same procedure as described in Scheme 1, which further were alkylated with appropriate alkyl halides to afford the N3-alkylated compounds (**19**).²⁴ At last, the final compounds **20a–f** were synthesized using the same synthetic methods as described above. And compounds **20g–l** were prepared by a method similar to that for compound **20a**.

Scheme 2

RESULTS AND DISCUSSION

Scaffold Hopping and Binding Mode Analysis. Through a structure-based design strategy targeting a hydrophobic sub-pocket induced by a gatekeeper mutant T790M, compound **7** (Figure 2A) was previously identified as a nanomolar irreversible EGFR inhibitor with a double-mutant selective profile (IC₅₀ against EGFR^{L858R/T790M} kinase over EGFR^{WT} kinase: 4.7 nM vs 474 nM, 101-fold selectivity).²⁵ After superimposing the docked pose of compound **7** with another double-mutant-selective EGFR inhibitor **5** (Figure 2B), the binding mode of both double-mutant inhibitors share some similar characteristics: 1) The aminopyrimidine moiety of both inhibitors binds to Met793 residue at the hinge region through two hydrogen bonding

1
2
3 interactions. 2) The hydrophilic tail on the left-hand side faces toward solvent-exposure area. 3)
4
5 The warhead, meta-acrylamide group, forms a covalent bond with Cys797. Besides, there are
6
7 two sub-pockets induced by gatekeeper mutant T790M (Figure 2C). Based on the overlaid
8
9 docked poses of compounds **5** and **7**, sub-pocket 1 (S1) is occupied by the fluorine group in the
10
11 C5-CF₃ substituent of compound **5** or the methyl group at N5-position of compound **7**,
12
13 respectively. In order to further improve the selectivity profile, by occupying both mutant-
14
15 induced sub-pockets (S1 and S2), compound **14a** was designed with a novel scaffold:
16
17 pyrimido[4,5-*d*]pyrimidine-2,4(1*H*,3*H*)-dione. According to the docked pose of compound **14a**
18
19 (Figure 2D), the carbonyl group at C4-position occupies the S1 pocket as well, like compounds **5**
20
21 and **7**. And hydrophobic groups with different lengths and volumes at the R³ position could be
22
23 introduced to explore the S2 pocket and to strengthen the nonpolar contacts with the gatekeeper
24
25 mutant Met790.
26
27
28
29
30

31 **Structure-activity Relationship.** **14a** inhibited the enzymatic activity against
32
33 EGFR^{L858R/T790M} and EGFR^{WT} with IC₅₀ values of 46 and 180 nM, respectively, and showed
34
35 nearly 4-fold selectivity for EGFR^{L858R/T790M} in comparison with EGFR^{WT} (Table 1). Its *in vitro*
36
37 antiproliferation activity were tested by using the sulforhodamine B (SRB) colorimetric assay on
38
39 H1975 cell lines (expressing EGFR-L858R/T790M) and A431 cell lines (harboring over-
40
41 expressed EGFR^{WT}). However, it exhibited weak antiproliferative effects on both the H1975 and
42
43 A431 cell lines (> 10 μM). Thus, we decided to improve the physical properties of **14a** by
44
45 exploring the R² position. With a *N,N*-dimethylpiperidin-4-amine substituent at the R² position
46
47 (compound **14d**), the predicted cell permeability score was improved from 64.1 (**14a**) to 80.3
48
49 (**14d**) (the higher value, the better cell permeability, predicted by Qikprop in Maestro software
50
51 package²⁶). As we expected, the enzymatic activity of **14d** against EGFR kinases and the
52
53
54
55
56
57
58
59
60

1
2
3 selectivity between EGFR^{L858R/T790M} and EGFR^{WT} remain the same level as **14a** (Table 1).
4
5 Besides, compound **14d** displayed potent inhibitory activity against H1975 cell line (230 nM),
6
7 and showed selectivity against the H1975 over the A431 cell lines (approximately 17-fold). As a
8
9 contrast, we also synthesized compound **14e** with no modification on R¹ and R². As expected,
10
11 **14e** lost the selectivity between EGFR^{L858R/T790M} and EGFR^{WT}, and showed weak
12
13 antiproliferative effects on both the H1975 and A431 cell lines (> 9 μM). The results once again
14
15 verify the importance of the hydrophilic tail on the left-hand side. Since compound **14d** showed
16
17 better inhibitory activity at both enzymatic and cellular levels, and acceptable aqueous solubility
18
19 (531 μg/mL), it was selected as a new starting point for the next-round structure modifications.
20
21
22
23

24 **Table 1**

25
26
27
28
29
30
31 Based on the strategy we described in Figure 2D, probing the S2 pocket is one of the most
32
33 important structure-based optimizations to improve the selectivity against double mutants over
34
35 wild type. Considering the feasibility of synthesis, hydrophobic groups with varied length and
36
37 volume were introduced at R³ position (Table 2). Thus, compounds **20a-f** were synthesized
38
39 (Scheme 2). When varying the substituted group at R³ position from methyl, ethyl, propyl to
40
41 isopropyl (compounds **14d**, **20a-c**), the enzymatic inhibition against double-mutant EGFR also
42
43 boosted correspondingly with the increase of group length and volume. For compounds **20b** and
44
45 **20c**, their values of IC₅₀ against double-mutant EGFR reach the subnanomolar range (0.4 and 0.8
46
47 nM, respectively, Table 2). Based on the docking simulation (Figure 2E), the hydrophobic
48
49 groups at R³ position is able to occupy the T790M mutant induced S2 pocket as well as
50
51 strengthen van der Waals (VDWs) contacts with gatekeeper Met790. Compared with the positive
52
53
54
55
56
57
58
59
60

1
2
3 control compound **5**, all three compounds (**20a-c**) showed a double-mutant preferred selectivity
4 (14-fold vs. 44, 33 and 25-fold), but the longer and bulkier substituents at R³ position
5
6 (compounds **20d-f**) keep potent inhibitory activity against double-mutant EGFR, these structural
7
8 modifications also increase the inhibition against wild-type EGFR, resulting in complete loss of
9
10 double-mutant selective profile (0.6, 0.7, 2.7-fold, respectively). There are many structures that
11
12 show the flexibility of S2 pocket to accommodate a wide range of hydrophobic moieties in both
13
14 EGFR double-mutant and wild-type structures.^{27,28} According to our docking simulations,
15
16 compound **20f** is able to be docked into both double-mutant and wild-type EGFR structures with
17
18 a wide open S2 pocket (Figure 2F and Figure S1). Based on the docked pose of **20f** with double-
19
20 mutant EGFR, we believe that the energy gain from occupying at S2 pocket with bulkier group
21
22 compensates the steric strain (1.9 Å: the distance in Figure 2F shows unfavorable VDW
23
24 interactions) between the carbonyl group at C4-position and wild type gatekeeper Thr790. Thus,
25
26 compounds with longer and bulkier substituents at R³ position regain inhibitory activity against
27
28 wild-type EGFR. At the second-round optimization, compounds **20a-c** also showed a better
29
30 selectivity against H1975 cell lines over A431 cell lines than that of compounds **20d-f** (12, 11
31
32 and 4-fold, respectively). This trend is in consistent with that at the enzymatic level.
33
34
35
36
37
38
39
40

41 At the third round, we moved forward with the most selective one at cellular level (**20c**) for
42
43 further structural optimizations. Previously, some literatures have also reported to modify the
44
45 left-hand side chain of the compounds to discovery active candidates.²⁹⁻³¹ Inspired by that, we
46
47 synthesized a set of compounds (compounds **20g-l**) that possess different left-hand side chains
48
49 on the basis of **20c** (Table 2). The data revealed that compounds **20h**, **20j-l** displayed varying
50
51 degrees selectivity losses in EGFR enzymatic inhibitory activity compared with **20c**.
52
53 Encouragingly, compounds **20g** and **20i** demonstrated more potent selectivity for double-mutant
54
55
56
57
58
59
60

1
2
3 EGFR enzyme (263-fold and 34-fold, respectively) and increase of aqueous solubility (262
4 $\mu\text{g/mL}$ and $280 \mu\text{g/mL}$, respectively) than **20c**. Especially **20g**, which showed 263-fold
5
6 selectivity between the EGFR^{L858R/T790M} and the EGFR^{WT}, and showed more potent inhibitory
7
8 activity and selectivity than the positive control compound **5**. In consistent with their enzyme
9
10 inhibitory activity, these compounds also showed different results in antiproliferation assays.
11
12 Compounds **20g-i** were roughly equipotent to **20c** for the H1975 cell lines, but resulted in
13
14 varying degrees drops of selectivity for A431 cells, especially **20h** and **20i**. And **20j-l** exhibited
15
16 diminished antiproliferation activity for H1975 cells and increased antiproliferation efficiency
17
18 for A431 cells as compared to **20c** (Table 2).
19
20
21
22
23

24
25 **Table 2**
26
27
28
29
30

31 **Inhibitory Effects of EGFR and Downstream Signaling Transduction.** The selective
32
33 inhibition of the representative compound **20g** for the phosphorylation of EGFR and the
34
35 downstream signaling transduction was further confirmed by using the Western blot analysis
36
37 (Figure 3). In H1975 cells, **20g** inhibited the phosphorylation of EGFR^{L858R/T790M} at the
38
39 concentration as low as 1 nM, and potently inhibited EGFR phosphorylation and downstream
40
41 molecules AKT phosphorylation at 100 nM, which even showed more potent inhibitory activity
42
43 relative to compound **6** (Figure 3A). In A431 cells, **20g** moderately inhibited the phosphorylation
44
45 of EGFR^{WT} even at 100 nM (Figure 3B). The results clearly showed that compound **20g** more
46
47 potently inhibited the phosphorylation of EGFR and downstream signaling transduction (p-AKT)
48
49 in cellular level, further suggesting **20g** was a potent and selective EGFR^{L858R/T790M} inhibitor.
50
51
52
53
54

55 **Figure 3**
56
57
58
59
60

1
2
3
4
5
6
7 **Target Duration of Action of Compound 20g in Vitro.** In order to get an insight into the
8 duration of target inhibition *in vitro*, we performed washout experiment. Compound **20g** was
9 washed out after incubation for 2 h in H1975 cells. Then phosphorylation of target at different
10 time points was detected by Western blot. As shown in Figure 4A, inhibition of target
11 EGFR^{L858R/T790M} activation can last for 24 h at least. And inhibition of the signaling protein ERK
12 activation can also last for more than 12 h. Furthermore, the target duration was similar to that of
13 control compound **6** (Figure 4B).
14
15
16
17
18
19
20
21

22 **Figure 4**

23
24
25
26
27
28 **DMPK Properties of Compound 20g.** In the permeability properties assay, compound **20g**
29 showed modest permeability in the MDCK II cells ($P_{app, A \rightarrow B}$ of 1.5×10^{-6} cm/s, and P_{app} ratio of
30 9.1 at 2 μ M). We then examined the *in vitro* metabolic stability of compound **20g** with human
31 and mouse liver microsomes. At the assay concentration of 0.1 μ M, the results demonstrated that
32 **20g** exhibited acceptable microsomal stability with half-life ($T_{1/2}$) of 85.4 min (human liver
33 microsomes) and 46.1 min (mouse liver microsomes), and MF% of 44.3 and 49.4, respectively
34 (Table S1). In addition, **20g** showed weak cytochrome P450 (CYP450) inhibition against five
35 major human CYP450 enzymes (1A2, 2C9, 2C19, and 2D6: $IC_{50} > 50$ μ M; 3A4: $IC_{50} = 23.9$
36 μ M). We also examined the preliminary *in vivo* pharmacokinetic properties of compound **20g** in
37 mice following intravenous (IV) and oral administration. As shown in Table 3, **20g** demonstrated
38 a reasonable area under the curve ($AUC_{0-\infty}$) value of 658 ng·h/mL, moderate half-life ($T_{1/2} = 1.1$ h)
39 and oral bioavailability ($F = 35\%$) during the oral dose of 10 mg/kg. The results indicate that it is
40 meaningful to further evaluate the preliminary *in vivo* antitumor efficacy studies of compound
41
42
43
44
45
46
47
48
49
50
51
52
53
54
55
56
57
58
59
60

1
2
3 **20g.**
4
5

6 **Table 3**
7
8
9

10
11 **In Vivo Antitumor Efficiency Study.** On the basis of its outstanding *in vitro* inhibitory
12 activity, we selected compound **20g** to further evaluate its preliminary *in vivo* antitumor efficacy
13 in H1975 and A431 xenograft mouse models (Figure 5). In this study, 4-6 weeks-old mice (n =
14 6/group) in treatment group were dosed orally once daily with **20g** at 50 mg/kg for 14 days. As
15 shown in Figure 5A, compared with the vehicle group, **20g** significantly inhibited the tumor
16 growth (TGI = 73%, $p < 0.001$) during the 14 day period in H1975 xenograft mouse mode.
17 However, **20g** exhibited much less potent tumor growth inhibition (TGI = 37%, $p < 0.05$) in A431
18 xenograft mouse model (Figure 5B). Besides, during the experiment, no significant body weight
19 loss, mortality and obvious side effects were observed (Figure 5C and 5D), indicating that
20 compound **20g** was well-tolerated at this dose.
21
22
23
24
25
26
27
28
29
30
31
32
33

34
35 **Figure 5**
36
37
38
39
40

41 CONCLUSIONS

42
43
44
45 Through a 3D conformer based scaffold hopping protocol based on previously reported mutant-
46 selective EGFR inhibitors, we designed and synthesized a series of pyrimido[4,5-*d*]pyrimidine-
47 2,4(1*H*,3*H*)-dione derivatives as novel potent and selective EGFR^{L858R/T790M} inhibitors. For three
48 compounds (**20b**, **20c** and **20g**) in this series, our design strategy to occupy S2 pocket boosts the
49 inhibitions against double-mutant EGFR and brings the IC₅₀ to a subnanomolar level. After three
50
51
52
53
54
55
56
57
58
59
60

1
2
3 round SAR explorations, one of the most promising compounds **20g** shows a favorable
4 selectivity at both *in vitro* and *in vivo* levels, indicating that compound **20g** might be used as a
5 promising drug candidate to overcome EGFR^{L858R/T790M} drug-resistance mutation. Further
6 evaluation for the candidate compound is still ongoing, and will be reported in due course.
7
8
9
10
11
12
13
14
15

16 EXPERIMENTAL SECTION

17
18
19 **Molecular Modeling.** The X-ray structures (PDB code: 3IKA and 4G5J) were downloaded
20 from the Protein Data Bank (PDB, <http://www.pdb.org>). The protocol of comparative docking
21 study was reported in our previous publications²³: First, compounds **5** and **7** was docked into the
22 EGFR^{T790M} (PDB code: 3IKA) as reversible inhibitors using Glide²³ (version 5.5) in extra
23 precision (XP) mode with default settings; Then, the covalent bond between the Cys797 and the
24 electrophilic group was formed by the build panel in Maestro²⁶; Finally, to fix the bond lengths
25 and eliminate steric clashed, the inhibitor-kinase covalent complex was minimized in water
26 solvent using MacroModel application with a flexible ligand and a restrained protein.
27
28
29
30
31
32
33
34
35
36
37

38
39 The scaffold hopping was conducted by an in-house software: SHAFTS³². The query molecule
40 is the docked pose of compound **7** obtained from the above docking study. The aligned pose of
41 compound **20c** (similarity score is 1.2875) was generated by a fast 3D-similarity calculation in
42 SHAFTS³³. Then, formed the covalent bond and minimized complexes with MacroModel
43 application with the same settings as described above.
44
45
46
47
48
49
50

51 For getting docked poses of compound **20f** with wild-type and double-mutant EGFRs. Two
52 structures (PDB code: 2RGP and 3W2S) were prepared in Maestro and aligned to the structure
53 with PDB code 3IKA. Compound **20f** (similarity score is 1.4038) was aligned to the docked pose
54
55
56
57
58
59
60

1
2
3 of compound 7 by SHAFTS. Then manually formed the covalent bond and minimized in
4
5 MacroModel.
6

7
8 **Reagents and General Methods.** All chemical reagents and solvents used in experiments
9
10 were purchased from commercial suppliers and used without further purification. Silica gel
11
12 (300–400 mesh) used for column chromatography and thin-layer chromatography (TLC) used to
13
14 monitor progress of the reaction were purchased from Qingdao Haiyang Chemical Co.,Ltd. ^1H
15
16 and ^{13}C NMR spectra were performed on the Bruker spectrometer (AV-400) at 400 MHz and
17
18 100 MHz, respectively. The low-resolution mass spectra (LC-MS) were measured using Agilent
19
20 6120 LC-MS. The high-resolution mass spectra (HRMS, Waters LCT Premier XE TOF) were
21
22 measured at the Institute of Fine Chemistry of ECUST. Melting points were determined with the
23
24 digital melting point apparatus (WRS-1B). The purity of final compounds were analyzed by
25
26 HPLC (Hewlett-Packard 1100), with the purity of all compounds being over than 95%. The
27
28 HPLC instrument was equipped with a photodiode array detector using a Zorbax RP-18 column
29
30 (5 μm , 4.6 mm \times 250 mm, reverse phase column). The mobile phases A and B were acetonitrile
31
32 and the solution of 10 mM ammonium acetate in purified water (pH = 6.0), respectively.
33
34
35
36
37
38

39 ***tert*-Butyl(3-Aminophenyl)carbamate (8).** To a mixture of 1,3-phenylenediamine (10.800 g,
40
41 100 mmol), Et_3N (10.100 g, 100 mmol) in methanol (150 mL) was added Boc_2O (21.800 g, 100
42
43 mmol) at 0 $^\circ\text{C}$. The reaction solution was stirred for 24 h at room temperature. Then, the solution
44
45 was concentrated with a rotary evaporator. The crude product was purified by silica gel
46
47 chromatography (petroleum ether/ethylacetate = 4:1, v/v) to obtain the title compound 2 as white
48
49 powder (13.310 g, 64%). ^1H NMR (400 MHz, CDCl_3) δ 7.03 (t, J = 8.0 Hz, 1H), 6.96 (s, 1H),
50
51 6.55 (dd, J = 8.0 Hz, J = 1.2 Hz, 1H), 6.43 (s, 1H), 6.36 (dd, J = 8.0 Hz, J = 1.6 Hz, 1H), 3.54 (s,
52
53 2H), 1.51 (s, 9H). LC-MS: m/z : 209.1 ($\text{M}+\text{H}$) $^+$.
54
55
56
57
58
59
60

Ethyl-4-((3-((*tert*-butoxycarbonyl)amino)phenyl)amino)-2-chloropyrimidine-5-

carboxylate (9). A mixture of ethyl-2,4-dichloropyrimidine-5-carboxylate (2.210 g, 10 mmol), compound **8** (2.080 g, 10 mmol) and DIPEA (1.935 g, 15 mmol) in CH₃CN (40 mL) was heated with reflux for 2 h. After cooling to room temperature, the white solid was collected by filtration and washed with CH₃CN to give the product **9** (3.371 g, 86%). ¹H NMR (400 MHz, DMSO-*d*₆) δ 10.23 (s, 1H), 9.50 (s, 1H), 8.80 (s, 1H), 7.70 (s, 1H), 7.35 (d, *J* = 7.6 Hz, 1H), 7.29 (t, *J* = 8.0 Hz, 1H), 7.24 (d, *J* = 8.4 Hz, 1H), 4.39 (q, *J* = 7.2 Hz, 2H), 1.49 (s, 9H), 1.36 (t, *J* = 7.2 Hz, 3H). LC-MS: *m/z*: 393.1 (M+H)⁺.

4-((3-((*tert*-Butoxycarbonyl)Amino)phenyl)amino)-2-chloropyrimidine-5-carboxylic acid

(10). A mixture of compound **9** (3.136 g, 8 mmol) in THF and 1 M NaOH (8 mL) was heated at 50 °C for 3 h. After cooling to room temperature, the solution was acidified with 1 M HCl to give a white solid, which was collected by filtration and washed with THF and water to give the title compound **10** (2.796 g, 96%). ¹H NMR (400 MHz, DMSO-*d*₆) δ 10.84 (s, 1H), 9.49 (s, 1H), 8.76 (s, 1H), 7.67 (s, 1H), 7.40 (d, *J* = 8.0 Hz, 1H), 7.28 (t, *J* = 8.0 Hz, 1H), 7.22 (d, *J* = 8.4 Hz, 1H), 1.49 (s, 9H). LC-MS: *m/z*: 365.1 (M+H)⁺.

4-((3-((*tert*-Butoxycarbonyl)Amino)phenyl)amino)-2-(phenylamino)pyrimidine-5-

carboxylic acid (11). To a solution of compound **10** (2.184 g, 6 mmol) in CH₃CN (40 mL) was added aniline (0.558 g, 6 mmol), the mixture was heated with reflux for 12 h. After cooling to room temperature, the residue was collected by filtration and washed with CH₃CN to give the product **11** as a white solid (2.249 g, 89%). ¹H NMR (400 MHz, DMSO-*d*₆) δ 10.44 (s, 1H), 9.82 (s, 1H), 9.36 (s, 1H), 8.70 (s, 1H), 7.69 (d, *J* = 8.0 Hz, 2H), 7.63 (s, 1H), 7.43 (s, 1H), 7.26-7.21 (m, 4H), 6.98 (t, *J* = 6.8 Hz, 1H), 1.47 (s, 9H). HRMS(ESI) (*m/z*): (M+H)⁺ calcd for C₂₂H₂₄N₅O₄ 422.1828, found, 422.1823.

***tert*-Butyl(3-((5-(Methylcarbamoyl)-2-(phenylamino)pyrimidin-4-yl)amino)phenyl)carbamate (12).** To a solution of **11** (1.263 g, 3 mmol), DIPEA (0.774 g, 6 mmol) in dry DMF (15 mL) was added HATU (1.368 g, 3.6 mmol). After stirring for 1 h at room temperature, methylamine hydrochloride (0.306 g, 4.5 mmol) was added and stirred overnight. The reaction mixture was poured into ice water, the resulting solid was collected by filtration, washed with water and recrystallized from EtOH to give the product **12** (0.612 g, 47%). ¹H NMR (400 MHz, DMSO-*d*₆) δ 11.33 (s, 1H), 9.59 (s, 1H), 9.31 (s, 1H), 8.64 (s, 1H), 8.50 (d, *J* = 4.8 Hz, 1H), 7.69 (d, *J* = 7.6 Hz, 2H), 7.62 (s, 1H), 7.50-7.48 (m, 1H), 7.23 (t, *J* = 7.6 Hz, 2H), 7.19 (d, *J* = 8.0 Hz, 1H), 7.15 (d, *J* = 8.0 Hz, 1H), 6.96 (t, *J* = 7.2 Hz, 1H), 2.79 (d, *J* = 4.4 Hz, 3H), 1.47 (s, 9H). LC-MS: *m/z*: 435.2 (M+H)⁺.

***tert*-Butyl(3-(3-Methyl-2,4-dioxo-7-(phenylamino)-3,4-dihydropyrimido[4,5-*d*]pyrimidin-1(2*H*)-yl)phenyl)carbamate (13).** To a solution of **12** (0.434 g, 1 mmol), K₂CO₃ (0.276 g, 2 mmol) in dry THF (10 mL) was added 1,1'-carbonyldiimidazole (0.324 g, 2 mmol). The reaction mixture was heated with reflux overnight. After cooling to room temperature, the reaction mixture was poured into water, and extracted with CH₂Cl₂ (3×20 mL). The organic layer was washed with saturated aqueous NaCl, dried over anhydrous Na₂SO₄ and concentrated in vacuo. The residue was purified by silica gel chromatography (petroleum ether/ethylacetate = 1:2, v/v) to give the product **13** as a white solid (0.193 g, 42%). ¹H NMR (400 MHz, DMSO-*d*₆) δ 9.62 (s, 1H), 8.92 (s, 1H), 7.66 (s, 1H), 7.52 (d, *J* = 8.0 Hz, 1H), 7.45 (t, *J* = 8.0 Hz, 1H), 7.36-7.32 (m, 2H), 7.03 (d, *J* = 8.0 Hz, 3H), 6.91 (d, *J* = 7.2 Hz, 1H), 3.30 (s, 3H), 1.45 (s, 9H). HRMS(ESI) (*m/z*): (M+H)⁺ calcd for C₂₄H₂₅N₆O₄ 461.1937, found, 461.1939.

***N*-(3-(3-Methyl-2,4-dioxo-7-(phenylamino)-3,4-dihydropyrimido[4,5-*d*]pyrimidin-1(2*H*)-yl)phenyl)acrylamide (14e).** To a solution of **13** (0.190 g, 0.41 mmol) in CH₂Cl₂ (4 mL) was

1
2
3 added trifluoroacetic acid (1 mL). The mixture was stirred for 4 h at room temperature. The
4
5 reaction solution was neutralized with saturated aqueous NaHCO₃, and extracted with CH₂Cl₂
6
7 (3×15 mL). The organic layer was washed with saturated aqueous NaCl, dried over anhydrous
8
9 Na₂SO₄ and concentrated in vacuo to obtain a white solid (0.136 g, 90%), which was used in the
10
11 next reaction without further purification.
12
13

14
15 To a solution of 1-(3-aminophenyl)-3-methyl-7-(phenylamino)pyrimido[4,5-*d*] pyrimidine-
16
17 2,4(1*H*,3*H*)-dione (0.136 g, 0.38 mmol) in NMP (1.5 mL) was added acryloyl chloride (37 μL,
18
19 0.46 mmol) dissolved in CH₃CN (0.5 mL) at 0 °C. The reaction solution was stirred overnight at
20
21 room temperature. The mixture was poured into water, and extracted with CH₂Cl₂ (3×15 mL).
22
23 The organic layer was washed with saturated aqueous NaCl, dried over anhydrous Na₂SO₄ and
24
25 concentrated in vacuo. The residue was purified by silica gel chromatography (petroleum
26
27 ether/ethylacetate = 1:1.5, v/v) to give the product **14e** as a white solid (0.083 g, 53%). mp
28
29 290.3-291.2 °C. ¹H NMR (400 MHz, DMSO-*d*₆) δ 10.38 (s, 1H), 8.93 (s, 1H), 7.82 (d, *J* = 3.2
30
31 Hz, 1H), 7.80 (s, 1H), 7.53 (t, *J* = 8.0 Hz, 1H), 7.33-7.29 (m, 2H), 7.15 (d, *J* = 7.6 Hz, 1H), 7.02-
32
33 6.96 (m, 2H), 6.89 (t, *J* = 6.0 Hz, 1H), 6.44 (dd, *J* = 17.2 Hz, *J* = 10.4 Hz, 1H), 6.25 (dd, *J* = 17.2
34
35 Hz, *J* = 1.6 Hz, 1H), 5.76 (dd, *J* = 10.4 Hz, *J* = 2.0 Hz, 1H), 3.30 (s, 3H). ¹³C NMR (100 MHz,
36
37 DMSO-*d*₆) δ 163.24, 160.11, 158.97, 157.87, 150.86, 139.90, 138.91, 136.19, 131.61, 129.45,
38
39 128.11, 127.22, 124.30, 122.53, 120.07, 119.26, 119.07, 27.57. HRMS(ESI) (*m/z*): (*M*+*H*)⁺
40
41 calcd for C₂₂H₁₉N₆O₃ 415.1519, found, 415.1512. HPLC purity: 97.66%, retention time = 10.68
42
43 min.
44
45
46
47
48
49

50
51 The following compounds **14a-d** were prepared by a method similar to that for the synthesis
52
53 of compound **14e**.
54
55
56
57
58
59
60

1
2
3 ***N*-(3-(7-((4-(4-Acetylpiperazin-1-yl)-2-methoxyphenyl)amino)-3-methyl-2,4-dioxo-3,4-**
4 **dihydropyrimido[4,5-*d*]pyrimidin-1(2*H*)-yl)phenyl)acrylamide (14a).** Yellow solid (yield
5 49%). mp 228.5-229.8 °C. ¹H NMR (400 MHz, DMSO-*d*₆) δ 10.34 (s, 1H), 8.83 (s, 1H), 8.59 (s,
6 1H), 7.86 (s, 1H), 7.69 (s, 1H), 7.48 (t, *J* = 8.4 Hz, 1H), 7.18 (d, *J* = 8.8 Hz, 1H), 7.09 (d, *J* = 8.0
7 Hz, 1H), 6.55 (s, 1H), 6.45 (dd, *J* = 17.2 Hz, *J* = 10.4 Hz, 1H), 6.26 (dd, *J* = 17.2 Hz, *J* = 1.6 Hz,
8 1H), 5.99 (s, 1H), 5.77 (dd, *J* = 10.0 Hz, *J* = 1.2 Hz, 1H), 3.76 (s, 3H), 3.58-3.54 (m, 4H), 3.28
9 (s, 3H), 3.05-2.99 (m, 4H), 2.05 (s, 3H). ¹³C NMR (100 MHz, DMSO-*d*₆) δ 168.19, 163.21,
10 160.10, 157.83, 139.73, 135.99, 131.67, 129.33, 127.18, 49.15, 48.76, 45.42, 40.60, 27.54, 21.16.
11 HRMS(ESI) (m/z): (M+H)⁺ calcd for C₂₉H₃₁N₈O₅ 571.2417, found, 571.2417. HPLC purity:
12 97.63%, retention time = 9.50 min.
13
14
15
16
17
18
19
20
21
22
23
24
25

26
27 ***N*-(3-(7-((2-Methoxy-4-morpholinophenyl)amino)-3-methyl-2,4-dioxo-3,4-**
28 **dihydropyrimido[4,5-*d*]pyrimidin-1(2*H*)-yl)phenyl)acrylamide (14b).** Yellow solid (yield
29 51%). mp >300 °C. ¹H NMR (400 MHz, DMSO-*d*₆) δ 10.36 (s, 1H), 8.80 (s, 1H), 8.44 (s, 1H),
30 8.03 (s, 1H), 7.86 (d, *J* = 8.0 Hz, 1H), 7.69 (t, *J* = 2.0 Hz, 1H), 7.52 (t, *J* = 8.4 Hz, 1H), 7.32 (d, *J*
31 = 8.8 Hz, 1H), 7.09 (d, *J* = 7.6 Hz, 1H), 6.57 (d, *J* = 2.0 Hz, 1H), 6.45 (dd, *J* = 16.8 Hz, *J* = 10.0
32 Hz, 1H), 6.27 (dd, *J* = 17.2 Hz, *J* = 2.0 Hz, 1H), 5.77 (dd, *J* = 10.4 Hz, *J* = 2.0 Hz, 1H), 3.77 (s,
33 3H), 3.58-3.54 (m, 4H), 3.06-2.99 (m, 4H), 2.05 (s, 3H). ¹³C NMR (100 MHz, DMSO-*d*₆) δ
34 163.23, 160.09, 158.87, 157.82, 150.86, 149.81, 148.06, 139.74, 135.98, 131.65, 129.34, 127.19,
35 124.18, 121.08, 120.00, 119.12, 105.61, 99.65, 99.15, 66.03, 55.64, 48.78, 27.54. HRMS(ESI)
36 (m/z): (M+H)⁺ calcd for C₂₇H₂₈N₇O₅ 528.1995, found, 528.1993. HPLC purity: 96.86%,
37 retention time = 10.73 min.
38
39
40
41
42
43
44
45
46
47
48
49
50
51
52

53 ***N*-(3-(7-((2-Methoxy-4-thiomorpholinophenyl)amino)-3-methyl-2,4-dioxo-3,4-**
54 **dihydropyrimido[4,5-*d*]pyrimidin-1(2*H*)-yl)phenyl)acrylamide (14c).** Yellow solid (yield
55
56
57
58
59
60

52%). mp 246.0-247.1 °C. ¹H NMR (400 MHz, DMSO-*d*₆) δ 10.35 (s, 1H), 8.84 (s, 1H), 8.60 (s, 1H), 8.85 (s, 1H), 7.70 (s, 1H), 7.48 (t, *J* = 8.0 Hz, 1H), 7.17 (d, *J* = 8.4 Hz, 1H), 7.09 (d, *J* = 7.6 Hz, 1H), 6.45 (dd, *J* = 17.2 Hz, *J* = 10.0 Hz, 1H), 6.27 (dd, *J* = 16.8 Hz, *J* = 2.0 Hz, 1H), 5.97-5.95 (m, 1H), 5.77 (dd, *J* = 10.0 Hz, *J* = 1.6 Hz, 1H), 3.75 (s, 3H), 3.42-3.39 (m, 4H), 3.28 (s, 3H), 2.66-2.63 (m, 4H). ¹³C NMR (100 MHz, DMSO-*d*₆) δ 163.24, 160.08, 158.90, 157.81, 150.86, 149.99, 139.76, 135.99, 131.63, 129.33, 127.22, 124.19, 121.32, 120.01, 119.10, 106.85, 100.43, 99.63, 55.65, 51.46, 27.54, 25.62. HRMS(ESI) (*m/z*): (*M*+*H*)⁺ calcd for C₂₇H₂₈N₇O₄S 546.1923, found, 546.1924. HPLC purity: 95.21%, retention time = 12.49 min.

***N*-(3-(7-((4-(4-(Dimethylamino)piperidin-1-yl)-2-methoxyphenyl)amino)-3-methyl-2,4-dioxo-3,4-dihydropyrimido[4,5-*d*]pyrimidin-1(2*H*)-yl)phenyl)acrylamide (14d)**. Yellow solid (yield 47%). mp >300 °C. ¹H NMR (400 MHz, DMSO-*d*₆) δ 10.36 (s, 1H), 8.83 (s, 1H), 8.54 (s, 1H), 7.88-7.86 (m, 1H), 7.70 (s, 1H), 7.47 (t, *J* = 8.0 Hz, 1H), 7.16 (d, *J* = 8.4 Hz, 1H), 7.08 (d, *J* = 7.6 Hz, 1H), 6.50-6.43 (m, 2H), 6.26 (dd, *J* = 16.8 Hz, *J* = 1.6 Hz, 1H), 5.98-5.96 (m, 1H), 5.76 (dd, *J* = 10.0 Hz, *J* = 1.2 Hz, 1H), 3.75 (s, 3H), 3.59-3.58 (m, 2H), 3.28 (s, 3H), 2.60-2.55 (m, 2H), 2.22 (s, 6H), 1.81 (d, *J* = 7.6 Hz, 2H), 1.47-1.40 (m, 2H). HRMS(ESI) (*m/z*): (*M*+*H*)⁺ calcd for C₃₀H₃₅N₈O₄ 571.2781, found, 571.2780. HPLC purity: 97.96%, retention time = 11.35 min.

2,4-Dichloropyrimidine-5-carboxamide (15). To a solution of 2,4-dichloropyrimidine-5-carbonyl chloride (4.220 g, 20 mmol) in dichloromethane (15 mL) was added ammonium hydroxide (1.400 g, 40 mmol) at 0 °C. The reaction mixture was stirred for 2 h at 0 °C, and the mixture was poured into ice water. The resulting solid was collected by filtration, washed with water to give the product **15** as a white solid (3.510 g, 92%). ¹H NMR (400 MHz, DMSO-*d*₆) δ 8.91 (s, 1H), 8.20 (s, 1H), 8.08 (s, 1H).

***tert*-Butyl(3-((5-Carbamoyl-2-chloropyrimidin-4-yl)amino)phenyl)carbamate (16).** A mixture of compound **15** (3.438 g, 18 mmol), DIPEA (3.483 g, 27 mmol), compound **8** (3.744 g, 18 mmol) in isopropanol (50 mL) was heated at 40 °C for 5 h. After cooling to room temperature, the white solid was collected by filtration and washed with isopropanol to give the product **16** (5.480 g, 84%). ¹H NMR (400 MHz, DMSO-*d*₆) δ 11.51 (s, 1H), 9.49 (s, 1H), 8.78 (s, 1H), 8.47 (s, 1H), 8.00 (s, 1H), 7.64 (s, 1H), 7.41 (d, *J* = 8.0 Hz, 1H), 7.27 (t, *J* = 8.0 Hz, 1H), 7.20 (d, *J* = 8.0 Hz, 1H), 1.48 (s, 9H). LC-MS: *m/z*: 364.1 (M+H)⁺.

***tert*-Butyl(3-((5-Carbamoyl-2-((4-(4-(dimethylamino)piperidin-1-yl)-2-methoxyphenyl)amino)pyrimidin-4-yl)amino)phenyl)carbamate (17).** To a mixture of compound **16** (5.082 g, 14 mmol), trifluoroacetic acid (1.550 mL, 21 mmol) in isopropanol (100 mL) was added 1-(4-amino-3-methoxyphenyl)-*N,N*-dimethylpiperidin-4-amine (4.183 g, 16.8 mmol). The reaction solution was heated with reflux overnight. After cooling to room temperature, the solution was concentrated with a rotary evaporator. And neutralized with saturated aqueous NaHCO₃, extracted with CH₂Cl₂ (3×50 mL). The organic layer was washed with saturated aqueous NaCl, dried over anhydrous Na₂SO₄ and concentrated in vacuo. The residue was purified by silica gel chromatography (dichloromethane/methanol = 15:1, v/v) to give the product **17** (5.450 g, 67%). ¹H NMR (400 MHz, DMSO-*d*₆) δ 11.46 (s, 1H), 9.34 (s, 1H), 8.65 (s, 1H), 8.24 (s, 1H), 8.08 (s, 1H), 7.52 (d, *J* = 8.8 Hz, 1H), 7.41 (d, *J* = 7.6 Hz, 1H), 7.37 (s, 1H), 7.12-7.07 (m, 2H), 6.62 (d, *J* = 1.6 Hz, 1H), 6.45 (d, *J* = 8.4 Hz, 1H), 3.77 (s, 3H), 3.70 (d, *J* = 12.0 Hz, 2H), 2.66 (t, *J* = 11.2 Hz, 2H), 2.20 (s, 6H), 1.84 (d, *J* = 12.0 Hz, 2H), 1.54-1.49 (m, 2H), 1.47 (s, 9H). LC-MS: *m/z*: 577.4 (M+H)⁺.

***tert*-Butyl(3-(7-((4-(4-(Dimethylamino)piperidin-1-yl)-2-methoxyphenyl)amino)-2,4-dioxo-3,4-dihydropyrimido[4,5-*d*]pyrimidin-1(2*H*)-yl)phenyl)carbamate (18).** A mixture of

1
2
3 compound **17** (5.184 g, 9 mmol), K₂CO₃ (1.863 g, 13.5 mmol), 1,1'-carbonyldiimidazole (2.916
4 g, 18 mmol) in dry THF (40 mL) was heated with reflux overnight. After cooling to room
5 temperature, the solution was added ice water and extracted with CH₂Cl₂ (3×30 mL). The
6 organic layer was washed with saturated aqueous NaCl, dried over anhydrous Na₂SO₄ and
7 concentrated in vacuo. The residue was purified by silica gel chromatography
8 (dichloromethane/methanol = 12:1, v/v) to give the product **18** (3.289 g, 60%). ¹H NMR (400
9 MHz, DMSO-*d*₆) δ 11.55 (s, 1H), 9.59 (s, 1H), 8.77 (s, 1H), 8.54 (s, 1H), 7.53 (s, 2H), 7.38 (t, *J*
10 = 8.0 Hz, 1H), 7.17 (d, *J* = 6.8 Hz, 1H), 6.96 (d, *J* = 7.2 Hz, 1H), 6.50 (s, 1H), 6.02-5.99 (m, 1H),
11 3.76 (s, 3H), 3.61-3.59 (m, 2H), 2.62-2.57 (m, 2H), 2.19 (s, 6H), 1.82 (d, *J* = 12.0 Hz, 2H), 1.51-
12 1.48 (m, 2H), 1.46 (s, 9H). LC-MS: *m/z*: 603.3 (M+H)⁺.
13
14
15
16
17
18
19
20
21
22
23
24
25
26

27 ***tert*-Butyl(3-(7-((4-(4-(Dimethylamino)piperidin-1-yl)-2-methoxyphenyl)amino)-3-ethyl-**
28 **2,4-dioxo-3,4-dihydropyrimido[4,5-*d*]pyrimidin-1(2*H*)-yl)phenyl)carbamate (**19**). To a
29 mixture of compound **18** (0.602 g, 1 mmol), Cs₂CO₃ (0.489 g, 1.5 mmol) in DMF (5 mL) was
30 added iodoethane (95 μL, 1.2 mmol). The mixture was stirred at room temperature overnight.
31 The solution was added ice water and extracted with CH₂Cl₂ (3×25 mL). The organic layer was
32 washed with saturated aqueous NaCl, dried over anhydrous Na₂SO₄ and concentrated in vacuo.
33 The residue was purified by silica gel chromatography (dichloromethane/methanol = 13:1, v/v)
34 to give the title compound **19** (0.378 g, 60%). ¹H NMR (400 MHz, DMSO-*d*₆) δ 9.60 (s, 1H),
35 8.83 (s, 1H), 8.58 (s, 1H), 7.57 (s, 1H), 7.53-7.51 (m, 1H), 7.39 (t, *J* = 7.6 Hz, 1H), 7.18 (d, *J* =
36 7.6 Hz, 1H), 6.97 (d, *J* = 7.2 Hz, 1H), 6.51 (s, 1H), 6.03-6.01 (m, 1H), 3.93 (q, *J* = 6.4 Hz, 2H),
37 3.76 (s, 3H), 3.63-3.60 (m, 2H), 2.63-2.58 (m, 2H), 2.24 (s, 6H), 1.83 (d, *J* = 12.0 Hz, 2H), 1.52-
38 1.47 (m, 2H), 1.46 (s, 9H), 1.17 (t, *J* = 6.8 Hz, 3H). LC-MS: *m/z*: 631.3 (M+H)⁺.
39
40
41
42
43
44
45
46
47
48
49
50
51
52
53
54
55
56
57
58
59
60**

1
2
3 ***N*-(3-(7-((4-(4-(Dimethylamino)piperidin-1-yl)-2-methoxyphenyl)amino)-3-ethyl-2,4-**
4 **dioxo-3,4-dihydropyrimido[4,5-*d*]pyrimidin-1(2*H*)-yl)phenyl)acrylamide (20a).** To a
5 solution of compound **19** (0.348 g, 0.55 mmol) in CH₂Cl₂ (5 mL) was added trifluoroacetic acid
6 (1.5 mL). The mixture was stirred for 5 h at room temperature. The reaction solution was
7 neutralized with saturated aqueous NaHCO₃, and extracted with CH₂Cl₂ (3×30 mL). The organic
8 layer was washed with saturated aqueous NaCl, dried over anhydrous Na₂SO₄ and concentrated
9 in vacuo to obtain a yellow solid (0.241 g, 82%), which was used in the next reaction without
10 further purification.
11
12
13
14
15
16
17
18
19
20
21

22 To a solution of 1-(3-aminophenyl)-7-((4-(4-(dimethylamino)piperidin-1-yl)-2-
23 methoxyphenyl)amino)-3-ethylpyrimido[4,5-*d*]pyrimidine-2,4(1*H*,3*H*)-dione (0.220 g, 0.4
24 mmol) in NMP (1.5 mL) was added acryloyl chloride (42 μL, 0.5 mmol) dissolved in CH₃CN
25 (0.5 mL) at 0 °C. The reaction solution was stirred overnight at room temperature. The mixture
26 was poured into water, and extracted with CH₂Cl₂ (3×20 mL). The organic layer was washed
27 with saturated aqueous NaCl, dried over anhydrous Na₂SO₄ and concentrated in vacuo. The
28 residue was purified by silica gel chromatography (dichloromethane/methanol = 12:1, v/v) to
29 give the title product **20a** as a yellow solid (0.116 g, 49%). mp 212.1-213.6 °C. ¹H NMR (400
30 MHz, DMSO-*d*₆) δ 10.64 (s, 1H), 10.56 (s, 1H), 8.84 (s, 1H), 8.62 (s, 1H), 7.92-7.90 (m, 1H),
31 7.71 (s, 1H), 7.48 (t, *J* = 8.0 Hz, 1H), 7.17 (d, *J* = 6.8 Hz, 1H), 7.10 (d, *J* = 7.2 Hz, 1H), 6.55-6.49
32 (m, 2H), 6.28 (dd, *J* = 16.8 Hz, *J* = 1.6 Hz, 1H), 6.00 (s, 1H), 5.78 (dd, *J* = 11.2 Hz, *J* = 1.2 Hz,
33 1H), 3.94 (q, *J* = 6.4 Hz, 2H), 3.76 (s, 3H), 3.72-3.68 (m, 2H), 2.73 (s, 6H), 2.60 (t, *J* = 8.0 Hz,
34 1H), 2.63-2.58 (m, 2H), 2.09 (d, *J* = 11.2 Hz, 2H), 1.72-1.68 (m, 2H), 1.18 (t, *J* = 6.4 Hz, 3H).
35 HRMS(ESI) (*m/z*): (*M*+*H*)⁺ calcd for C₃₁H₃₇N₈O₄ 585.2938, found, 585.2928. HPLC purity:
36 96.26%, retention time = 9.95 min.
37
38
39
40
41
42
43
44
45
46
47
48
49
50
51
52
53
54
55
56
57
58
59
60

The following compounds **20b-1** were prepared by a synthesis route similar to that for compound **20a**.

***N*-(3-(7-((4-(4-(Dimethylamino)piperidin-1-yl)-2-methoxyphenyl)amino)-2,4-dioxo-3-propyl-3,4-dihydropyrimido[4,5-*d*]pyrimidin-1(2*H*)-yl)phenyl)acrylamide (20b)**. Yellow solid (yield 39%). mp >300 °C. ¹H NMR (400 MHz, DMSO-*d*₆) δ 10.54 (s, 1H), 8.84 (s, 1H), 8.63 (s, 1H), 7.92 (s, 1H), 7.69 (s, 1H), 7.49 (t, *J* = 8.0 Hz, 1H), 7.19 (d, *J* = 6.8 Hz, 1H), 7.10 (d, *J* = 7.8 Hz, 1H), 6.54-6.48 (m, 2H), 6.28 (dd, *J* = 16.8 Hz, *J* = 1.2 Hz, 1H), 6.00 (s, 1H), 5.78 (dd, *J* = 10.4 Hz, *J* = 1.6 Hz, 1H), 3.86 (t, *J* = 6.8 Hz, 2H), 3.76 (s, 3H), 3.72-3.69 (m, 2H), 3.26-3.21 (m, 1H), 2.72 (s, 6H), 2.62-2.57 (m, 2H), 2.07 (d, *J* = 11.2 Hz, 2H), 1.70-1.67 (m, 2H), 1.65-1.60 (m, 2H), 0.90 (t, *J* = 7.2 Hz, 3H). HRMS(ESI) (*m/z*): (M+H)⁺ calcd for C₃₂H₃₉N₈O₄ 599.3094, found, 599.3099. HPLC purity: 97.85%, retention time = 10.96 min.

***N*-(3-(7-((4-(4-(Dimethylamino)piperidin-1-yl)-2-methoxyphenyl)amino)-3-isopropyl-2,4-dioxo-3,4-dihydropyrimido[4,5-*d*]pyrimidin-1(2*H*)-yl)phenyl)acrylamide (20c)**. Yellow solid (yield 41%). mp >300 °C. ¹H NMR (400 MHz, DMSO-*d*₆) δ 10.55 (s, 1H), 8.83 (s, 1H), 8.60 (s, 1H), 7.91 (s, 1H), 7.69 (s, 1H), 7.48 (t, *J* = 8.0 Hz, 1H), 7.19 (d, *J* = 5.6 Hz, 1H), 7.10 (d, *J* = 7.6 Hz, 1H), 6.55-6.48 (m, 2H), 6.28 (dd, *J* = 17.2 Hz, *J* = 1.6 Hz, 1H), 6.00 (s, 1H), 5.78 (dd, *J* = 10.0 Hz, *J* = 1.6 Hz, 1H), 5.17-5.10 (m, 1H), 3.76 (s, 3H), 3.72-3.68 (m, 2H), 3.26-3.20 (m, 1H), 2.72 (s, 6H), 2.63-2.59 (m, 2H), 2.07 (d, *J* = 10.8 Hz, 2H), 1.70-1.67 (m, 2H), 1.44 (d, *J* = 6.8 Hz, 6H). ¹³C NMR (100 MHz, DMSO-*d*₆) δ 163.29, 160.19, 157.83, 139.83, 135.83, 135.95, 131.81, 129.22, 127.00, 124.26, 120.04, 119.06, 106.58, 99.91, 62.21, 55.67, 47.77, 45.00, 25.55, 19.25. HRMS(ESI) (*m/z*): (M+H)⁺ calcd for C₃₂H₃₉N₈O₄ 599.3094, found, 599.3079. HPLC purity: 98.38%, retention time = 11.12 min.

1
2
3 ***N*-(3-(3-Benzyl-7-((4-(4-(dimethylamino)piperidin-1-yl)-2-methoxyphenyl)amino)-2,4-**
4 **dioxo-3,4-dihydropyrimido[4,5-*d*]pyrimidin-1(2*H*)-yl)phenyl)acrylamide (20d).** Yellow solid
5
6 (yield 39%). mp 285.4-286.6 °C. ¹H NMR (400 MHz, DMSO-*d*₆) δ 10.54 (s, 1H), 8.87 (s, 1H),
7
8 8.69 (s, 1H), 7.91 (s, 1H), 7.69 (s, 1H), 7.48 (t, *J* = 8.0 Hz, 1H), 7.38 (d, *J* = 7.2 Hz, 2H), 7.33 (t,
9
10 *J* = 7.2 Hz, 2H), 7.26 (t, *J* = 7.2 Hz, 1H), 7.19 (d, *J* = 8.0 Hz, 1H), 7.11 (d, *J* = 6.8 Hz, 1H), 6.54-
11
12 6.47 (m, 2H), 6.27 (dd, *J* = 16.8 Hz, *J* = 1.6 Hz, 1H), 6.01-5.99 (m, 1H), 5.77 (dd, *J* = 10.0 Hz, *J*
13
14 = 1.6 Hz, 1H), 5.10 (s, 2H), 3.76 (s, 3H), 3.72-3.69 (m, 2H), 3.27-3.21 (m, 1H), 2.73 (s, 6H),
15
16 2.62-2.57 (m, 2H), 2.08 (d, *J* = 11.2 Hz, 2H), 1.71-1.68 (m, 2H). ¹³C NMR (100 MHz, DMSO-
17
18 *d*₆) δ 163.31, 159.94, 139.88, 136.98, 135.84, 131.82, 129.27, 128.30, 127.63, 127.14, 127.01,
19
20 62.24, 59.74, 55.68, 47.72, 43.83, 25.47, 20.74. HRMS(ESI) (*m/z*): (M+H)⁺ calcd for
21
22 C₃₆H₃₉N₈O₄ 647.3094, found, 647.3088. HPLC purity: 95.30%, retention time = 12.72 min.
23
24
25
26
27
28

29 ***N*-(3-(7-((4-(4-(Dimethylamino)piperidin-1-yl)-2-methoxyphenyl)amino)-2,4-dioxo-3-**
30 **phenethyl-3,4-dihydropyrimido[4,5-*d*]pyrimidin-1(2*H*)-yl)phenyl)acrylamide (20e).** Yellow
31
32 solid (yield 40%). mp 196.5-197.7 °C. ¹H NMR (400 MHz, DMSO-*d*₆) δ 10.58 (s, 1H), 8.85 (s,
33
34 1H), 8.67 (s, 1H), 7.91 (s, 1H), 7.72 (s, 1H), 7.49 (t, *J* = 8.0 Hz, 1H), 7.32 (t, *J* = 7.6 Hz, 2H),
35
36 7.26-7.23 (m, 3H), 7.19 (d, *J* = 12.8 Hz, 1H), 7.07 (d, *J* = 6.8 Hz, 1H), 6.56-6.49 (m, 2H), 6.28
37
38 (dd, *J* = 17.2 Hz, *J* = 1.6 Hz, 1H), 6.01-5.99 (m, 1H), 5.78 (dd, *J* = 10.4 Hz, *J* = 1.6 Hz, 1H),
39
40 4.10-4.08 (m, 2H), 3.77 (s, 3H), 3.72-3.69 (m, 2H), 3.24-3.19 (m, 1H), 2.90 (t, *J* = 7.6 Hz, 2H),
41
42 2.71 (s, 6H), 2.62-2.57 (m, 2H), 2.07 (d, *J* = 11.2 Hz, 2H), 1.70-1.68 (m, 2H). ¹³C NMR (100
43
44 MHz, DMSO-*d*₆) δ 163.33, 159.68, 139.90, 138.51, 135.82, 131.83, 129.26, 128.59, 128.50,
45
46 127.02, 126.39, 62.23, 55.70, 47.74, 41.92, 33.28, 25.52. HRMS(ESI) (*m/z*): (M+H)⁺ calcd for
47
48 C₃₇H₄₁N₈O₄ 661.3251, found, 661.3251. HPLC purity: 99.09%, retention time = 13.71 min.
49
50
51
52
53
54
55
56
57
58
59
60

***N*-3-(7-((4-(4-(Dimethylamino)piperidin-1-yl)-2-methoxyphenyl)amino)-2,4-dioxo-3-(3-phenylpropyl)-3,4-dihydropyrimido[4,5-*d*]pyrimidin-1(2*H*)-yl)phenyl)acrylamide (20f).**

Yellow solid (yield 38%). mp 252.1-253.8 °C. ¹H NMR (400 MHz, DMSO-*d*₆) δ 10.72 (s, 1H), 8.81 (s, 1H), 8.60 (s, 1H), 7.92 (s, 1H), 7.78 (s, 1H), 7.48 (t, *J* = 8.0 Hz, 1H), 7.28-7.19 (m, 5H), 7.14 (t, *J* = 7.2 Hz, 1H), 7.07 (d, *J* = 7.2 Hz, 1H), 6.61-6.52 (m, 2H), 6.29 (dd, *J* = 17.2 Hz, *J* = 1.6 Hz, 1H), 6.02 (s, 1H), 5.78 (dd, *J* = 10.0 Hz, *J* = 1.6 Hz, 1H), 3.94 (t, *J* = 7.2 Hz, 2H), 3.76 (s, 3H), 3.22-3.17 (m, 1H), 2.69 (s, 6H), 2.68-2.63 (m, 4H), 2.08 (d, *J* = 10.4 Hz, 2H), 1.94 (t, *J* = 6.8 Hz, 2H). ¹³C NMR (100 MHz, DMSO-*d*₆) δ 163.33, 159.89, 157.82, 141.32, 139.88, 135.89, 131.84, 129.23, 128.21, 128.12, 126.99, 125.68, 62.20, 47.76, 40.52, 32.51, 28.57, 25.57. HRMS(ESI) (*m/z*): (*M*+*H*)⁺ calcd for C₃₈H₄₃N₈O₄ 675.3407, found, 675.3403. HPLC purity: 95.85%, retention time = 14.42 min.

***N*-3-(3-Isopropyl-7-((2-methoxy-4-(4-methylpiperazin-1-yl)phenyl)amino)-2,4-dioxo-3,4-dihydropyrimido[4,5-*d*]pyrimidin-1(2*H*)-yl)phenyl)acrylamide (20g).** Yellow solid (yield 39%). mp >300 °C. ¹H NMR (400 MHz, DMSO-*d*₆) δ 10.64 (s, 1H), 8.83 (s, 1H), 8.63 (s, 1H), 7.85 (d, *J* = 7.2 Hz, 1H), 7.73 (s, 1H), 7.47 (t, *J* = 8.0 Hz, 1H), 7.20 (d, *J* = 8.4 Hz, 1H), 7.09 (d, *J* = 7.6 Hz, 1H), 6.56-6.51 (m, 2H), 6.27 (dd, *J* = 17.2 Hz, *J* = 1.6 Hz, 1H), 6.03-6.01 (m, 1H), 5.77 (dd, *J* = 10.4 Hz, *J* = 1.2 Hz, 1H), 5.17-5.10 (m, 1H), 3.76 (s, 3H), 3.29 (t, *J* = 4.0 Hz, 4H), 3.20 (t, *J* = 4.0 Hz, 4H), 2.75 (s, 3H), 1.44 (d, *J* = 6.4 Hz, 6H). ¹³C NMR (100 MHz, DMSO-*d*₆) δ 163.33, 160.20, 157.83, 139.79, 135.94, 131.79, 129.21, 127.05, 120.09, 100.00, 55.74, 52.25, 46.05, 45.02, 42.29, 19.24. HRMS(ESI) (*m/z*): (*M*+*H*)⁺ calcd for C₃₀H₃₅N₈O₄ 571.2781, found, 571.2775. HPLC purity: 98.71%, retention time = 11.25 min.

***N*-3-(3-Isopropyl-7-((3-methoxy-4-(4-methylpiperazin-1-yl)phenyl)amino)-2,4-dioxo-3,4-dihydropyrimido[4,5-*d*]pyrimidin-1(2*H*)-yl)phenyl)acrylamide (20h).** Yellow solid (yield

1
2
3 47%). mp 221.3-222.5 °C. ¹H NMR (400 MHz, DMSO-*d*₆) δ 10.51 (s, 1H), 10.18 (s, 1H), 8.88
4 (s, 1H), 7.89 (s, 1H), 7.72 (s, 1H), 7.50 (t, *J* = 8.0 Hz, 1H), 7.13 (d, *J* = 8.0 Hz, 1H), 6.91 (s, 1H),
5
6 6.49 (dd, *J* = 16.8 Hz, *J* = 10.0 Hz, 1H), 6.43-6.41 (m, 1H), 6.27 (dd, *J* = 16.8 Hz, *J* = 1.6 Hz,
7
8 1H), 5.77 (dd, *J* = 10.0 Hz, *J* = 1.6 Hz, 1H), 5.18-5.11 (m, 1H), 3.56 (s, 3H), 3.04-3.01 (m, 8H),
9
10 2.63 (s, 3H), 1.44 (d, *J* = 6.8 Hz, 6H). ¹³C NMR (100 MHz, DMSO-*d*₆) δ 163.29, 160.17, 151.55,
11
12 150.38, 139.87, 136.09, 134.47, 131.73, 129.33, 127.13, 124.33, 120.10, 119.23, 55.29, 53.27,
13
14 47.95, 45.06, 43.21, 19.23. HRMS(ESI) (*m/z*): (*M*+*H*)⁺ calcd for C₃₀H₃₅N₈O₄ 571.2781, found,
15
16 571.2773. HPLC purity: 97.35%, retention time = 10.11 min.
17
18
19
20
21

22 ***N*-(3-(3-Isopropyl-7-((3-methyl-4-(4-methylpiperazin-1-yl)phenyl)amino)-2,4-dioxo-3,4-**
23 **dihydropyrimido[4,5-*d*]pyrimidin-1(2*H*)-yl)phenyl)acrylamide (20i).** Yellow solid (yield
24 49%). mp 295.5-296.9 °C. ¹H NMR (400 MHz, DMSO-*d*₆) δ 10.54 (s, 1H), 10.22 (s, 1H), 8.88
25
26 (s, 1H), 7.90 (d, *J* = 7.2 Hz, 1H), 7.74 (s, 1H), 7.51 (t, *J* = 8.0 Hz, 1H), 7.18 (s, 1H), 7.13 (d, *J* =
27
28 8.0 Hz, 1H), 7.08 (d, *J* = 6.4 Hz, 1H), 6.69 (d, *J* = 7.6 Hz, 1H), 6.50 (dd, *J* = 17.2 Hz, *J* = 10.4
29
30 Hz, 1H), 6.26 (dd, *J* = 17.2 Hz, *J* = 1.6 Hz, 1H), 5.76 (dd, *J* = 10.4 Hz, *J* = 1.6 Hz, 1H), 5.18-
31
32 5.11 (m, 1H), 3.12 (t, *J* = 4.0 Hz, 4H), 2.92 (t, *J* = 4.0 Hz, 4H), 2.70 (s, 3H), 1.97 (s, 3H), 1.44 (d,
33
34 *J* = 7.2 Hz, 6H). ¹³C NMR (100 MHz, DMSO-*d*₆) δ 163.29, 160.18, 159.05, 157.91, 150.40,
35
36 139.92, 136.16, 134.60, 132.03, 131.74, 129.37, 127.10, 124.26, 121.38, 119.95, 119.35, 118.62,
37
38 117.58, 53.35, 48.94, 45.04, 42.84, 19.23, 17.44. HRMS(ESI) (*m/z*): (*M*+*H*)⁺ calcd for
39
40 C₃₀H₃₅N₈O₃ 555.2832, found, 555.2831. HPLC purity: 99.05%, retention time = 10.93 min.
41
42
43
44
45
46
47
48

49 ***N*-(3-(7-((4-((2-(Dimethylamino)ethyl)(methyl)amino)-2-methoxyphenyl)amino)-3-**
50 **isopropyl-2,4-dioxo-3,4-dihydropyrimido[4,5-*d*]pyrimidin-1(2*H*)-yl)phenyl)acrylamide (20j).**
51 Yellow solid (yield 37%). mp 150.7-152.4 °C. ¹H NMR (400 MHz, CDCl₃) δ 8.94 (s, 1H), 8.45
52
53 (s, 1H), 7.95 (s, 1H), 7.83 (s, 1H), 7.68 (d, *J* = 8.0 Hz, 1H), 7.46 (t, *J* = 8.0 Hz, 1H), 7.35 (d, *J* =
54
55
56
57
58
59
60

1
2
3 8.8 Hz, 1H), 7.04 (d, $J = 7.6$ Hz, 1H), 6.38 (dd, $J = 16.8$ Hz, $J = 1.6$ Hz, 1H), 6.27-6.17 (m, 2H),
4
5 5.83 (dd, $J = 9.6$ Hz, $J = 1.6$ Hz, 1H), 5.69 (d, $J = 10.4$ Hz, 1H), 5.36-5.29 (m, 1H), 3.81 (s, 3H),
6
7 3.39 (t, $J = 7.6$ Hz, 2H), 2.88 (s, 3H), 2.45 (t, $J = 7.6$ Hz, 2H), 2.32 (s, 6H), 1.55 (d, $J = 6.8$ Hz,
8
9 6H). HRMS(ESI) (m/z): (M+H)⁺ calcd for C₃₀H₃₇N₈O₄ 573.2938, found, 573.2932. HPLC
10
11
12 purity: 95.07%, retention time = 10.56 min.
13
14

15 ***N*-(3-(7-((4-(2-(Dimethylamino)ethoxy)-2-methoxyphenyl)amino)-3-isopropyl-2,4-dioxo-**
16
17 **3,4-dihydropyrimido[4,5-*d*]pyrimidin-1(2*H*)-yl)phenyl)acrylamide (20k).** Yellow solid (yield
18
19 41%). mp 195.4-196.7 °C. ¹H NMR (400 MHz, DMSO-*d*₆) δ 10.39 (s, 1H), 8.84 (s, 1H), 8.64 (s,
20
21 1H), 7.80 (d, $J = 4.4$ Hz, 1H), 7.71 (s, 1H), 7.48 (t, $J = 8.0$ Hz, 1H), 7.23 (d, $J = 5.6$ Hz, 1H),
22
23 7.10 (d, $J = 7.6$ Hz, 1H), 6.52-6.42 (m, 2H), 6.27 (dd, $J = 17.2$ Hz, $J = 1.6$ Hz, 1H), 6.01-5.99 (m,
24
25 1H), 5.77 (dd, $J = 10.0$ Hz, $J = 1.2$ Hz, 1H), 5.15-5.11 (m, 1H), 3.95 (t, $J = 5.2$ Hz, 2H), 3.75 (s,
26
27 3H), 2.60 (t, $J = 5.2$ Hz, 2H), 2.22 (s, 6H), 1.44 (d, $J = 6.8$ Hz, 6H). ¹³C NMR (100 MHz,
28
29 DMSO-*d*₆) δ 163.19, 160.20, 159.16, 157.83, 155.23, 150.33, 139.68, 136.00, 131.65, 129.27,
30
31 127.16, 124.32, 121.37, 120.08, 119.10, 103.84, 100.07, 98.76, 65.73, 57.64, 55.73, 45.47, 44.99,
32
33 19.23. HRMS(ESI) (m/z): (M+H)⁺ calcd for C₂₉H₃₄N₇O₅ 560.2621, found, 560.2625. HPLC
34
35
36 purity: 98.57%, retention time = 8.78 min.
37
38
39
40

41 ***N*-(3-(3-Isopropyl-7-((2-methoxy-4-(4-(4-methylpiperazin-1-yl)piperidin-1-yl)phenyl)**
42
43 **amino)-2,4-dioxo-3,4-dihydropyrimido[4,5-*d*]pyrimidin-1(2*H*)-yl)phenyl)acrylamide (20l).**
44
45 Yellow solid (yield 43%). mp >300 °C. ¹H NMR (400 MHz, DMSO-*d*₆) δ 10.57 (s, 1H), 8.82 (s,
46
47 1H), 8.57 (s, 1H), 7.91 (s, 1H), 7.70 (s, 1H), 7.47 (t, $J = 8.0$ Hz, 1H), 7.18 (d, $J = 6.8$ Hz, 1H),
48
49 7.09 (d, $J = 7.6$ Hz, 1H), 6.56-6.49 (m, 2H), 6.27 (dd, $J = 16.8$ Hz, $J = 1.6$ Hz, 1H), 5.99-5.97 (m,
50
51 1H), 5.77 (dd, $J = 10.0$ Hz, $J = 1.6$ Hz, 1H), 5.17-5.10 (m, 1H), 3.76 (s, 3H), 3.64-3.61 (m, 2H),
52
53 2.96-2.75 (m, 6H), 2.60-2.56 (m, 6H), 1.87-1.85 (m, 1H), 1.54-1.50 (m, 2H), 1.44 (d, $J = 6.8$ Hz,
54
55
56
57
58
59
60

1
2
3 6H). ^{13}C NMR (100 MHz, $\text{DMSO-}d_6$) δ 163.31, 160.19, 159.07, 157.81, 150.34, 139.83, 135.92,
4
5 131.79, 129.22, 126.99, 119.99, 99.79, 60.77, 55.61, 52.86, 48.21, 46.52, 45.02, 43.23, 27.01,
6
7 19.24. HRMS(ESI) (m/z): (M+H) $^+$ calcd for $\text{C}_{35}\text{H}_{44}\text{N}_9\text{O}_4$ 654.3516, found, 654.3519. HPLC
8
9 purity: 99.38%, retention time = 11.76 min.
10
11
12

13 **In Vitro Enzymatic Inhibition and Cell Antiproliferation Activity Assay.** The enzymatic
14 inhibition and cell antiproliferation activity assays were evaluated by using the well-established
15 ELISA-based assay and sulforhodamine B (SRB) colorimetric assay, respectively. The detailed
16 experiments were performed according to the published literature,²⁵ and the detailed
17 characterizations are provided in the Supporting Information.
18
19
20
21
22
23
24

25 **Western Blot Analysis.** H1975 and A431 cells were collected and suspended in lysis buffer
26 (Tris-HCl, pH 6.8, 100 mmol/L; DTT, 200 mmol/L; 0.2% bromophenol blue; 4% SDS; 20%
27 glycerol). Equivalent amounts of proteins were loaded and separated by SDS-PAGE (8%), then
28 transferred to nitrocellulose membranes. Western blot analysis was subsequently performed with
29 standard procedures. The antibodies were used for immune detection of proteins, including p-
30 EGFR (Y1068; #3777S), EGFR (#4267S), p-AKT (Ser473), AKT, and GAPDH (Cell Signaling
31 Technologies, Cambridge, MA).
32
33
34
35
36
37
38
39
40
41

42 **Human and Mouse Liver Microsomal Stability Assays.** The incubation is performed as
43 follows: microsomes in 0.1 M Tris/HCl buffer of pH 7.4 (0.33 mg/mL microsomal protein), co-
44 factor MgCl_2 (5 mM), tested compound (final concentration of 0.1 μM , co-solvent (0.01%
45 DMSO) and 0.005% Bovin serum albumin) and NADPH (1 mM) at 37 °C for 60 min. The
46 reaction can be started by the addition of liver microsomes, or the tested compound or NADPH.
47
48
49
50
51
52
53
54 Aliquots were sampled at 0, 7, 17, 30 and 60 min incubation and enzymatic reaction is stopped
55
56
57
58
59
60

1
2
3 by protein precipitation in methanol. After centrifugation, samples are then analysed by LC-
4 MS/MS (Waters UPLC I-Class system; Xevo TQ-S mass spectrometer).
5
6

7
8 **Measurements of Aqueous Solubility, CYP Inhibition Assays, and Measurement of**
9 **Permeability.** Determination of the aqueous solubility was performed according to the published
10 literature.³⁴ The CYP inhibition assays and measurement of permeability of compound **20g** were
11 conducted by WuXi AppTec, and the detailed characterizations are provided in the Supporting
12 Information.
13
14
15
16
17
18
19
20

21 **In Vivo Pharmacokinetics Study in Mice.** The *in vivo* pharmacokinetic study in mice was
22 conducted by Shanghai Medicilon, Inc. Briefly, the dosing solution (1 mg/mL) was prepared by
23 dissolving the appropriate amount of the compound in 0.5% CMC-Na aqueous solution for oral
24 administration, and the 0.2 mg/mL dosing solution was prepared by dissolving the appropriate
25 amount of the compound in mixed solvent (0.15 mL DMSO+1.200 mL PEG400+1.650 mL
26 Saline) for intravenous administration. Male ICR mice were separately administered to some
27 groups (three mice /group) for oral (10 mg/kg) or intravenous (1 mg/kg) administration. At time
28 points 0.083, 0.25, 0.5, 1, 2, 4, 8, and 24 h after dosing, the blood sample was collected from
29 each animal and stored in 0–4 °C, then separated by centrifugation (8000 r/min for 6 min). All
30 samples were analyzed using LC–MS/MS (SIMADZU LC system; Applied Biosystems mass
31 spectrometer), and the acquired data were analyzed by using the WinNonlin (v5.2).
32
33
34
35
36
37
38
39
40
41
42
43
44
45
46

47 **In Vivo Antitumor Efficiency Study.** BALB/c mice (4-6 weeks-old) were purchased from
48 Shanghai Lab. Animal Research Center (Shanghai, China). Briefly, H1975 cell lines and A431
49 cell lines were cultured in RPMI-1640 (GE Healthcare) supplemented with 10% (v/v) fetal
50 bovine serum (Gibico). Then a total volume of 0.1 mL /mouse (approximately 2×10^6 cells) were
51
52
53
54
55
56
57
58
59
60

1
2
3 implanted subcutaneously into the right flank of the animals. When the size of the tumor reached
4
5 about 200–400 mm³, the mice were randomly divided into vehicle group and treated group (six
6
7 mice /group). For antitumor efficacy studies, mice were dosed once daily by oral administration
8
9 with vehicle or inhibitor with the indicated dose for 14 consecutive days. The average tumor
10
11 volume was measured every 2 or 3 days using vernier calipers, followed by calculated with the
12
13 formula $V = (L \times W^2)/2$, where L stands for length, and W stands for width. All the animal
14
15 experiments in this article, including animal handling, care and treatment were performed in
16
17 compliance with Agreement of the ethics committee on laboratory animal care and the
18
19 Guidelines for the Care and Use of Laboratory Animals in Shanghai, China.
20
21
22
23
24
25
26
27

28 ASSOCIATED CONTENT

31 Supporting Information

32
33
34 The docked pose of **20f**, and the metabolic stability of **20g** in human and mouse liver
35
36 microsomes are in the supporting material. Also include availability of molecular formula strings
37
38 (CSV). This material is available free of charge via the Internet at <http://pubs.acs.org>.
39
40
41

42 AUTHOR INFORMATION

45 Corresponding Authors

46
47 *E-mail: yfxu@ecust.edu.cn (Y.X.). Phone: +86-21-64251399.
48
49

50
51 *E-mail: hxie@jding.dhs.org (H.X.). Phone: +86-21-50805897.
52
53

54
55 *E-mail: hlli@ecust.edu.cn (H.L.). Phone/Fax: +86-21-64250213.
56
57
58
59
60

Author Contributions

‡These authors contributed equally.

Notes

The authors declare no competing financial interest.

ACKNOWLEDGMENTS

The research is supported in part by the National Key Research and Development Program (Grant 2016YFA0502304), the Shanghai Committee of Science and Technology (Grants 14431902100), Special Program for Applied Research on Super Computation of the NSFC-Guangdong Joint Fund (the second phase) under Grant No.U1501501. Honglin Li is also sponsored by National Program for Special Supports of Eminent Professionals and National Program for Support of Top-notch Young Professionals.

ABBREVIATIONS USED

EGFR, epidermal growth factor receptor; NSCLC, non-small cell lung cancer; WT, wild-type; TKIs, tyrosine kinase inhibitors; AKT, protein kinase B; ERK, extracellular signal-regulated kinases; TGI, tumor growth inhibition; DIPEA, *N,N*-diisopropylethylamine; CH₃CN, acetonitrile; HATU, 1-[Bis(dimethylamino)methylene]-1H-1,2,3-triazolo[4,5-b]pyridinium 3-oxid hexafluorophosphate; THF, tetrahydrofuran; DMF, *N,N*-dimethylformamide; NMP, 1-Methyl-2-pyrrolidinone

REFERENCES

- (1) Siegel, R.; Ward, E.; Brawley, O.; Jemal, A. Cancer statistics, 2011. *Ca-Cancer J. Clin.* **2011**, *61*, 212-236.
- (2) Yarden, Y.; Sliwkowski, M. X. Untangling the ErbB signalling network. *Nat. Rev. Mol. Cell Biol.* **2001**, *2*, 127-137.
- (3) Oda, K.; Matsuoka, Y.; Funahashi, A.; Kitano, H. A comprehensive pathway map of epidermal growth factor receptor signaling. *Mol. Syst. Biol.* **2005**, *1*, 1-17.
- (4) Peters, S.; Zimmermann, S.; Adjei, A. A. Oral epidermal growth factor receptor tyrosine kinase inhibitors for the treatment of non-small cell lung cancer: comparative pharmacokinetics and drug–drug interactions. *Cancer Treat. Rev.* **2014**, *40*, 917-926.
- (5) Cohen, M. H.; Williams, G. A.; Sridhara, R.; Chen, G.; McGuinn, W. D.; Morse, D.; Abraham, S.; Rahman, A.; Liang, C.; Lostritto, R.; Baird, A.; Pazdur, R. United states food and drug administration drug approval summary: gefitinib (ZD1839; Iressa) tablets. *Clin. Cancer Res.* **2004**, *10*, 1212-1218.
- (6) Cohen, M. H.; Johnson, J. R.; Chen, Y.-F.; Sridhara, R.; Pazdur, R. FDA drug approval summary: erlotinib (Tarceva®) tablets. *Oncologist.* **2005**, *10*, 461-466.
- (7) Cataldo, V. D.; Gibbons, D. L.; Pérez-Soler, R.; Quintás-Cardama, A. Treatment of non–small-cell lung cancer with erlotinib or gefitinib. *N. Engl. J. Med.* **2011**, *364*, 947-955.
- (8) Mitsudomi, T.; Morita, S.; Yatabe, Y.; Negoro, S.; Okamoto, I.; Tsurutani, J.; Seto, T.; Satouchi, M.; Tada, H.; Hirashima, T.; Asami, K.; Katakami, N.; Takada, M.; Yoshioka, H.; Shibata, K.; Kudoh, S.; Shimizu, E.; Saito, H.; Toyooka, S.; Nakagawa, K.; Fukuoka, M. Gefitinib versus cisplatin plus docetaxel in patients with non-small-cell lung cancer harbouring mutations of the epidermal growth factor receptor (WJTOG3405): an open label, randomised

1
2
3 phase 3 trial. *Lancet Oncol.* **2010**, *11*, 121-128.

4
5 (9) Rosell, R.; Carcereny, E.; Gervais, R.; Vergnenegre, A.; Massuti, B.; Felip, E.; Palmero, R.;
6
7 Garcia-Gomez, R.; Pallares, C.; Sanchez, J. M.; Porta, R.; Cobo, M.; Garrido, P.; Longo, F.;
8
9 Moran, T.; Insa, A.; De Marinis, F.; Corre, R.; Bover, I.; Illiano, A.; Dansin, E.; de Castro, J.;
10
11 Milella, M.; Reguart, N.; Altavilla, G.; Jimenez, U.; Provencio, M.; Moreno, M. A.; Terrasa, J.;
12
13 Muñoz-Langa, J.; Valdivia, J.; Isla, D.; Domine, M.; Molinier, O.; Mazieres, J.; Baize, N.;
14
15 Garcia-Campelo, R.; Robinet, G.; Rodriguez-Abreu, D.; Lopez-Vivanco, G.; Gebbia, V.; Ferrera-
16
17 Delgado, L.; Bombaron, P.; Bernabe, R.; Bearz, A.; Artal, A.; Cortesi, E.; Rolfo, C.; Sanchez-
18
19 Ronco, M.; Drozdowskyj, A.; Queralt, C.; de Aguirre, I.; Ramirez, J. L.; Sanchez, J. J.; Molina,
20
21 M. A.; Taron, M.; Paz-Ares, L. Erlotinib versus standard chemotherapy as first-line treatment for
22
23 european patients with advanced EGFR mutation-positive non-small-cell lung cancer
24
25 (EURTAC): a multicentre, open-label, randomised phase 3 trial. *Lancet Oncol.* **2012**, *13*, 239-
26
27 246.

28
29 (10) Yu, H. A.; Arcila, M. E.; Rekhman, N.; Sima, C. S.; Zakowski, M. F.; Pao, W.; Kris, M. G.;
30
31 Miller, V. A.; Ladanyi, M.; Riely, G. J. Analysis of tumor specimens at the time of acquired
32
33 resistance to EGFR-TKI therapy in 155 patients with EGFR-mutant lung cancers. *Clin. Cancer*
34
35 *Res.* **2013**, *19*, 2240-2247.

36
37 (11) Smaill, J. B.; Rewcastle, G. W.; Loo, J. A.; Greis, K. D.; Chan, O. H.; Reyner, E. L.; Lipka,
38
39 E.; Showalter, H. D. H.; Vincent, P. W.; Elliott, W. L.; Denny, W. A. Tyrosine kinase inhibitors.
40
41 irreversible inhibitors of the epidermal growth factor receptor: 4-(phenylamino)quinazoline- and
42
43 4-(phenylamino)pyrido[3,2-*d*]pyrimidine-6-acrylamides bearing additional solubilizing
44
45 functions. *J. Med. Chem.* **2000**, *43*, 1380-1397.

46
47 (12) Tsou, H.-R.; Overbeek-Klumpers, E. G.; Hallett, W. A.; Reich, M. F.; Floyd, M. B.;
48
49
50
51
52
53

1
2
3 Johnson, B. D.; Michalak, R. S.; Nilakantan, R.; Discafani, C.; Golas, J.; Rabindran, S. K.; Shen,
4 R.; Shi, X.; Wang, Y.-F.; Upeslakis, J.; Wissner, A. Optimization of 6,7-disubstituted-4-
5 (arylamino)quinoline-3-carbonitriles as orally active, irreversible inhibitors of human epidermal
6 growth factor receptor-2 kinase activity. *J. Med. Chem.* **2005**, *48*, 1107-1131.
7
8

9
10
11
12 (13) Engelman, J. A.; Zejnullahu, K.; Gale, C.-M.; Lifshits, E.; Gonzales, A. J.; Shimamura, T.;
13 Zhao, F.; Vincent, P. W.; Naumov, G. N.; Bradner, J. E.; Althaus, I. W.; Gandhi, L.; Shapiro, G.
14 I.; Nelson, J. M.; Heymach, J. V.; Meyerson, M.; Wong, K.-K.; Jänne, P. A. PF00299804, an
15 irreversible pan-ERBB inhibitor, is effective in lung cancer models with EGFR and ERBB2
16 mutations that are resistant to gefitinib. *Cancer Res.* **2007**, *67*, 11924-11932.
17
18
19

20
21
22 (14) Li, D.; Ambrogio, L.; Shimamura, T.; Kubo, S.; Takahashi, M.; Chirieac, L. R.; Padera, R.
23 F.; Shapiro, G. I.; Baum, A.; Himmelsbach, F.; Rettig, W. J.; Meyerson, M.; Solca, F.; Greulich,
24 H.; Wong, K. K. BIBW2992, an irreversible EGFR/HER2 inhibitor highly effective in preclinical
25 lung cancer models. *Oncogene* **2008**, *27*, 4702-4711.
26
27
28

29
30
31 (15) Dungo, R.; Keating, G. Afatinib: first global approval. *Drugs* **2013**, *73*, 1503-1515.
32

33
34 (16) Miller, V. A.; Hirsh, V.; Cadranel, J.; Chen, Y.-M.; Park, K.; Kim, S.-W.; Zhou, C.; Su, W.-
35 C.; Wang, M.; Sun, Y.; Heo, D. S.; Crino, L.; Tan, E.-H.; Chao, T.-Y.; Shahidi, M.; Cong, X. J.;
36 Lorence, R. M.; Yang, J. C.-H. Afatinib versus placebo for patients with advanced, metastatic
37 non-small-cell lung cancer after failure of erlotinib, gefitinib, or both, and one or two lines of
38 chemotherapy (LUX-lung 1): a phase 2b/3 randomised trial. *Lancet Oncology.* **2012**, *13*, 528-
39 538.
40
41
42

43
44 (17) Zhou, W.; Ercan, D.; Chen, L.; Yun, C.; Li, D.; Capelletti, M.; Cortot, A. B.; Chirieac, L.;
45 Iacob, R. E.; Padera, R.; Engen, J. R.; Wong, K.; Eck, M. J.; Gray, N. S.; Jänne, P. A. Novel
46 mutant-selective EGFR kinase inhibitors against EGFR T790M. *Nature.* **2009**, *462*, 1070-1074.
47
48
49
50
51
52
53
54
55
56
57
58
59
60

1
2
3 (18) Walter, A. O.; Sjin, R. T. T.; Haringsma, H. J.; Ohashi, K.; Sun, J.; Lee, K.; Dubrovskiy, A.;
4 Labenski, M.; Zhu, Z.; Wang, Z.; Sheets, M.; St Martin, T.; Karp, R.; van Kalken, D.;
5 Chaturvedi, P.; Niu, D.; Nacht, M.; Petter, R. C.; Westlin, W.; Lin, K.; Jaw-Tsai, S.; Raponi, M.;
6 Van Dyke, T.; Etter, J.; Weaver, Z.; Pao, W.; Singh, J.; Simmons, A. D.; Harding, T. C.; Allen, A.
7
8
9
10
11
12
13
14
15
16
17
18
19
20
21
22
23
24
25
26
27
28
29
30
31
32
33
34
35
36
37
38
39
40
41
42
43
44
45
46
47
48
49
50
51
52
53
54
55
56
57
58
59
60

Discovery of a mutant-selective covalent inhibitor of EGFR that overcomes T790M-mediated resistance in NSCLC. *Cancer Discovery*. **2013**, *3*, 1404-1415.

(19) Tjin Tham Sjin, R.; Lee, K.; Walter, A. O.; Dubrovskiy, A.; Sheets, M.; Martin, T. S.;
Labenski, M. T.; Zhu, Z.; Tester, R.; Karp, R.; Medikonda, A.; Chaturvedi, P.; Ren, Y.;
Haringsma, H.; Etter, J.; Raponi, M.; Simmons, A. D.; Harding, T. C.; Niu, D.; Nacht, M.;
Westlin, W. F.; Petter, R. C.; Allen, A.; Singh, J. In vitro and in vivo characterization of
irreversible mutant-selective EGFR inhibitors that are wild-type sparing. *Mol. Cancer Ther.*
2014, *13*, 1468-1479.

(20) Ward, R. A.; Anderton, M. J.; Ashton, S.; Bethel, P. A.; Box, M.; Butterworth, S.;
Colclough, N.; Chorley, C. G.; Chuaqui, C.; Cross, D. A. E.; Dakin, L. A.; Debreczeni, J. É.;
Eberlein, C.; Finlay, M. R. V.; Hill, G. B.; Grist, M.; Klinowska, T. C. M.; Lane, C.; Martin, S.;
Orme, J. P.; Smith, P.; Wang, F.; Waring, M. J. Structure- and reactivity-based development of
covalent inhibitors of the activating and gatekeeper mutant forms of the epidermal growth factor
receptor (EGFR). *J. Med. Chem.* **2013**, *56*, 7025-7048.

(21) Cross, D. A. E.; Ashton, S. E.; Ghiorghiu, S.; Eberlein, C.; Nebhan, C. A.; Spitzler, P. J.;
Orme, J. P.; Finlay, M. R. V.; Ward, R. A.; Mellor, M. J.; Hughes, G.; Rahi, A.; Jacobs, V. N.;
Brewer, M. R.; Ichihara, E.; Sun, J.; Jin, H.; Ballard, P.; Al-Kadhimi, K.; Rowlinson, R.;
Klinowska, T.; Richmond, G. H. P.; Cantarini, M.; Kim, D.-W.; Ranson, M. R.; Pao, W.
AZD9291, an irreversible EGFR TKI, overcomes T790M-mediated resistance to EGFR

1
2
3 inhibitors in lung cancer. *Cancer Discovery*. **2014**, *4*, 1046-1061.

4
5 (22) FDA approves new pill to treat certain patients with non-small cell lung cancer. November
6
7 13, 2015. <http://www.fda.gov/NewsEvents/Newsroom/PressAnnouncements/ucm472525.htm>.

8
9
10 (23) Hao Y.; Lyu J.; Qu R.; Sun D.; Zhao Z.; Chen, Z.; Ding, J.; Xie, H.; Xu, Y.; Li, H. Structure-
11
12 guided design of C4-alkyl-1,4-dihydro-2hpyrimido[4,5-*d*][1,3]oxazin-2-ones as potent and
13
14 mutant-selective epidermal growth factor receptor (EGFR) L858R/T790M inhibitors. *Scientific*
15
16 *Reports*. **2017**. *7*, 3830.

17
18
19 (24) Goto, S.; Tsuboi, H.; Kanoda, M.; Mukai, K.; Kagara, K. The process development of a
20
21 novel aldose reductase inhibitor, FK366. part 1. Improvement of discovery process and new
22
23 syntheses of 1-substituted quinazolinediones. *Org Process Res Dev*. **2003**, *7*, 700-706.

24
25
26 (25) Hao Y.; Wang X.; Zhang T.; Sun D.; Tong Y.; Xu Y.; Chen H.; Tong L.; Zhu L.; Zhao Z.;
27
28 Chen, Z.; Ding, J.; Xie, H.; Xu, Y.; Li, H. Discovery and structural optimization of N5-
29
30 substituted 6, 7-dioxo-6, 7-dihydropteridines as potent and selective epidermal growth factor
31
32 receptor (EGFR) inhibitors against L858R/T790M resistance mutation. *J Med Chem*. **2016**. *59*,
33
34 7111-7124.

35
36
37 (26) Maestro, version 9.0; Schrödinger, LLC: New York, NY, **2009**.

38
39
40 (27) Zhao, Z.; Wu, H.; Wang, L.; Liu, Y.; Knapp, S.; Liu, Q.; Gray, N. S. Exploration of type II
41
42 binding mode: a privileged approach for kinase inhibitor focused drug discovery? *ACS Chem*.
43
44 *Biol*. **2014**, *9*, 1230-1241.

45
46
47 (28) Roskoski, R. Classification of small molecule protein kinase inhibitors based upon the
48
49 structures of their drug-enzyme complexes. *Pharmacol. Res*. **2016**, *103*, 26-48.

50
51
52 (29) Chang, S.; Zhang, L.; Xu, S.; Luo, J.; Lu, X.; Zhang, Z.; Xu, T.; Liu, Y.; Tu, Z.; Xu, Y.; Ren,
53
54 X.; Geng, M.; Ding, J.; Pei, D.; Ding, K. Design, synthesis, and biological evaluation of novel
55
56
57
58
59
60

1
2
3 conformationally constrained inhibitors targeting epidermal growth factor receptor threonine790
4 → methionine790 mutant. *J. Med. Chem.* **2012**, *55*, 2711-2723.

7 (30) Zhou, W.; Liu, X.; Tu, Z.; Zhang, L.; Ku, X.; Bai, F.; Zhao, Z.; Xu, Y.; Ding, K.; Li, H.
8
9
10 Discovery of pteridin-7(8H)-one-based irreversible inhibitors targeting the epidermal growth
11 factor receptor (EGFR) kinase T790M/L858R mutant. *J. Med. Chem.* **2013**, *56*, 7821-7837.

14 (31) Xu, S.; Xu, T.; Zhang, L.; Zhang, Z.; Luo, J.; Liu, Y.; Lu, X.; Tu, Z.; Ren, X.; Ding, K.
15
16
17 Design, synthesis, and biological evaluation of 2-oxo-3,4-dihydropyrimido[4,5-*d*]pyrimidinyl
18 derivatives as new irreversible epidermal growth factor receptor inhibitors with improved
19 pharmacokinetic properties. *J. Med. Chem.* **2013**, *56*, 8803-8813.

23 (32) Liu, X.; Jiang, H.; Li, H. SHAFTS: a hybrid approach for 3D molecular similarity
24 calculation. 1. Method and assessment of virtual screening. *J. Chem. Inf. Model.* **2011**, *51*, 2372-
25
26
27
28
29 2385.

30 (33) Gong, J.; Cai, C.; Liu, X.; Ku, X.; Jiang, H.; Gao, D.; Li, H. ChemMapper: a versatile web
31 server for exploring pharmacology and chemical structure association based on molecular 3D
32 similarity method. *Bioinformatics.* **2013**, *29*, 1827-1829.

35 (34) Zhang, L.; Yuan, J.; Xu, Y.; Zhang, Y. H. P.; Qian, X. New artificial fluoro-cofactor of
36
37
38
39
40
41
42
43
44
45
46
47
48
49
50
51
52
53
54
55
56
57
58
59
60
hydride transfer with novel fluorescence assay for redox biocatalysis. *Chem. Commun.* **2016**, *52*,
6471-6474.

FIGURE CAPTIONS

Figure 1. Structures of representative first-, second- and third-generation EGFR inhibitors.

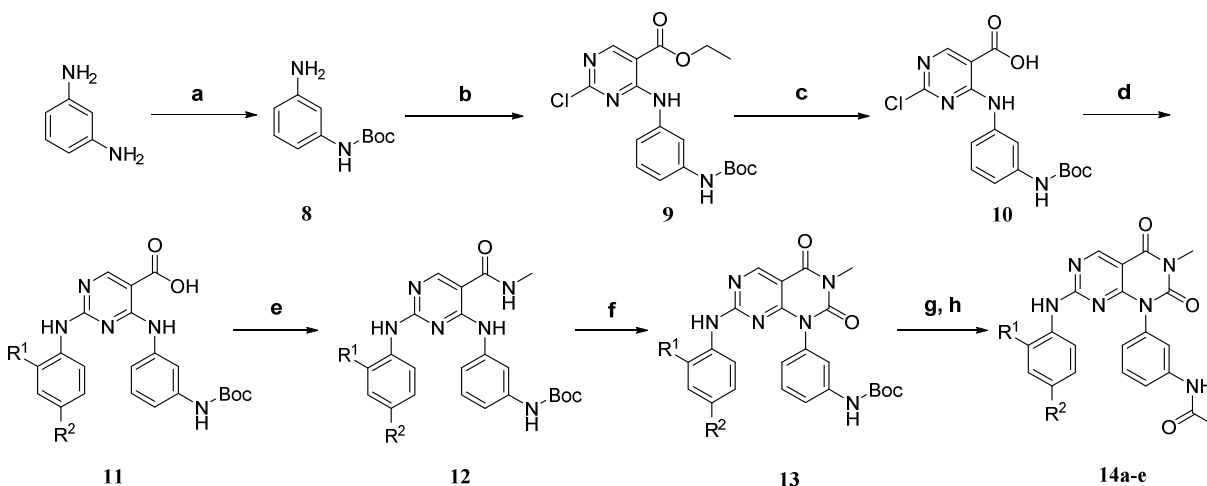
Figure 2. A) The 2D drawings of compound **5** and **7**; B) The overlaid docked poses of **5** (shown in orange sticks) and **7** (shown in blue sticks). The gatekeeper, hinge and covalent regions of both wild-type (PDB ID: 4G5J) and double-mutant (PDB ID: 3IKA) EGFR kinases are displayed in yellow sticks and cyan sticks, respectively; C) The sliced view of the predicted binding mode of **14a**. The docked pose of compound **14a** is in yellow sticks. The key residues Met793 and Met790 are shown in cyan sticks. The rest of the protein is demonstrated in a surface mode (PDB ID: 3IKA). D) The 2D interactions of the new scaffold to show strategies of structural modifications. E) The docked pose of compound **20c**. The protein (PDB ID: 3IKA) is shown in a blue cartoon and the key residues are shown in blue sticks. Key H-bond and VDW interactions are measured by distances. F) The docked pose of compound **20f**. The compound **20f** is in orange sticks. The mesh surface is shown to display the shape of the binding site and the S2 pocket. The key residues in the covalent, hinge and S2-pocket regions of both wild-type (PDB ID: 2RGP) and double-mutant (PDB ID: 3W2S) EGFR kinases are displayed in cyan sticks and green sticks, respectively

Figure 3. Inhibitory effects of compound **20g** for EGFR and downstream signaling transduction in H1975 cells (A) and A431 cells (B).

1
2
3 **Figure 4.** Target duration *in vitro*. NCI-H1975 cells were treated with **20g** (A) or compound **6** (B)
4
5 for 2 hours, then washed with PBS for 3 times. Target inhibition at different time points was
6
7 detected by Western blot.
8
9

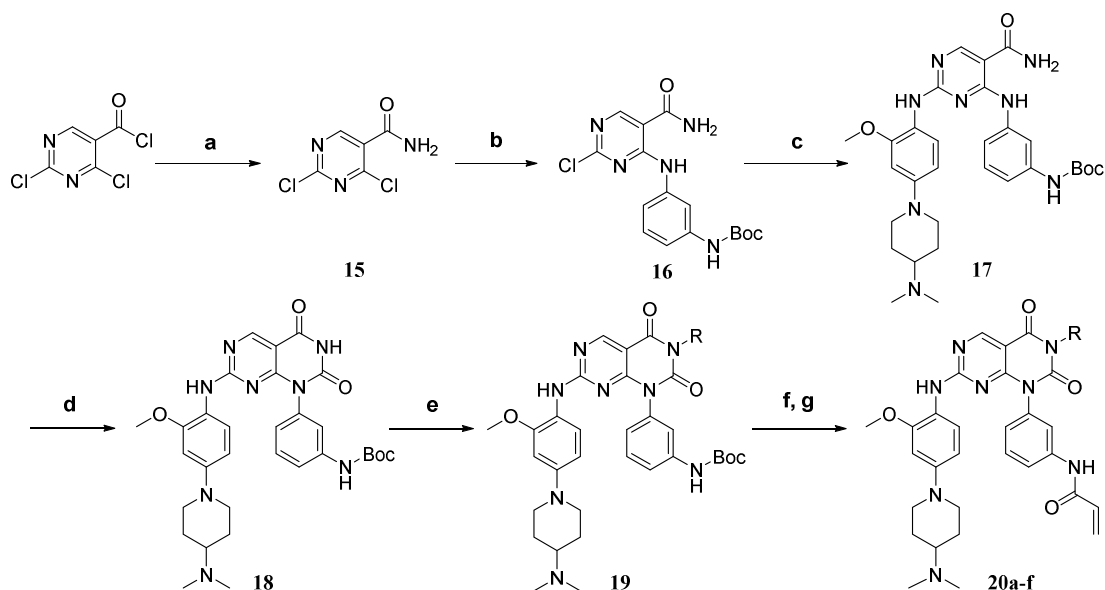
10
11
12
13
14 **Figure 5.** Preliminary *in vivo* antitumor efficiency study of compound **20g** (50 mg/kg/day)
15
16 against H1975 and A431 NSCLC xenograft mouse models. (A) H1975 xenograft mouse model
17
18 (n = 6) tumor volumes and (C) body weights, (B) A431 xenograft mouse model (n = 6) tumor
19
20 volumes and (D) body weights were recorded every 2-3 days. All values expressed as mean
21
22 \pm SEM. (*) $p < 0.05$ or (***) $p < 0.001$ (Student's *t* test) vs the vehicle group.
23
24
25
26
27
28
29
30
31
32
33
34
35
36
37
38
39
40
41
42
43
44
45
46
47
48
49
50
51
52
53
54
55
56
57
58
59
60

SCHEMES

Scheme 1. Synthesis of Pyrimido[4,5-*d*]pyrimidine-2,4(1*H*,3*H*)-dione Derivatives 14a-e^a

^aReagents and conditions: (a) (Boc)₂O, Et₃N, CH₃OH, r.t., 24 h, 64%; (b) ethyl 2,4-dichloropyrimidine-5-carboxylate, DIPEA, CH₃CN, reflux, 2 h, 86%; (c) 1M NaOH, THF, 50 °C, 3 h, 96%; (d) arylamine, CH₃CN, reflux, overnight, 42-89%; (e) methylamine hydrochloride, HATU, DIPEA, dry DMF, r.t., overnight, 31-47%; (f) 1,1'-carbonyldiimidazole, K₂CO₃, dry THF, reflux, overnight, 35-42%; (g) trifluoroacetic acid, CH₂Cl₂, r.t., 4 h, 81-90%; (h) acrylyl chloride, NMP/CH₃CN, 0 °C to r.t., overnight, 47-53%.

Scheme 2. Synthesis of Pyrimido[4,5-*d*]pyrimidine-2,4(1*H*,3*H*)-dione Derivatives 20a-f^a

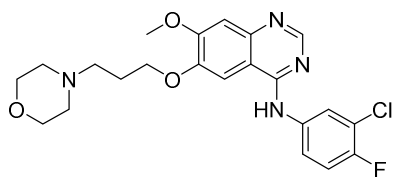


^aReagents and conditions: (a) ammonium hydroxide, CH₂Cl₂, 0 °C, 2 h, 92%; (b) *tert*-butyl(3-aminophenyl)carbamate, DIPEA, isopropanol, 40 °C, 5 h, 84%; (c) arylamine, trifluoroacetic acid, isopropanol, reflux, overnight, 67%; (d) 1,1'-carbonyldiimidazole, K₂CO₃, dry THF, reflux, overnight, 60%; (e) haloalkane, Cs₂CO₃, DMF, r.t., overnight, 55-61%; (f) trifluoroacetic acid, CH₂Cl₂, r.t., 5 h, 78-82%; (g) acrylyl chloride, NMP/CH₃CN, 0 °C to r.t., overnight, 37-49%.

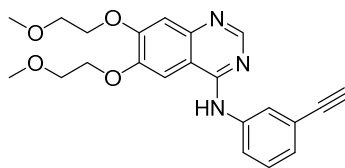
FIGURES

Figure 1

First-generation

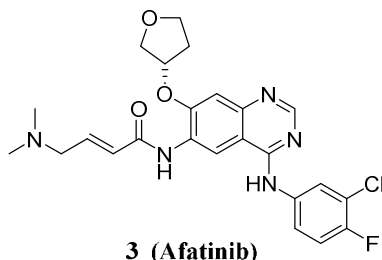


1 (Gefitinib)



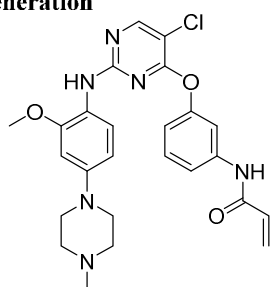
2 (Erlotinib)

Second-generation

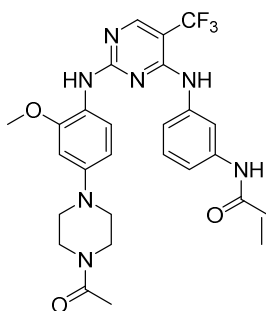


3 (Afatinib)

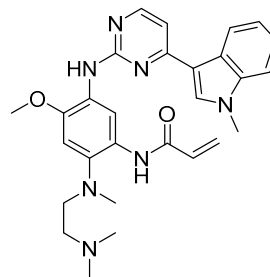
Third-generation



4 (WZ4002)



5 (CO-1686)



6 (AZD9291)

Figure 2

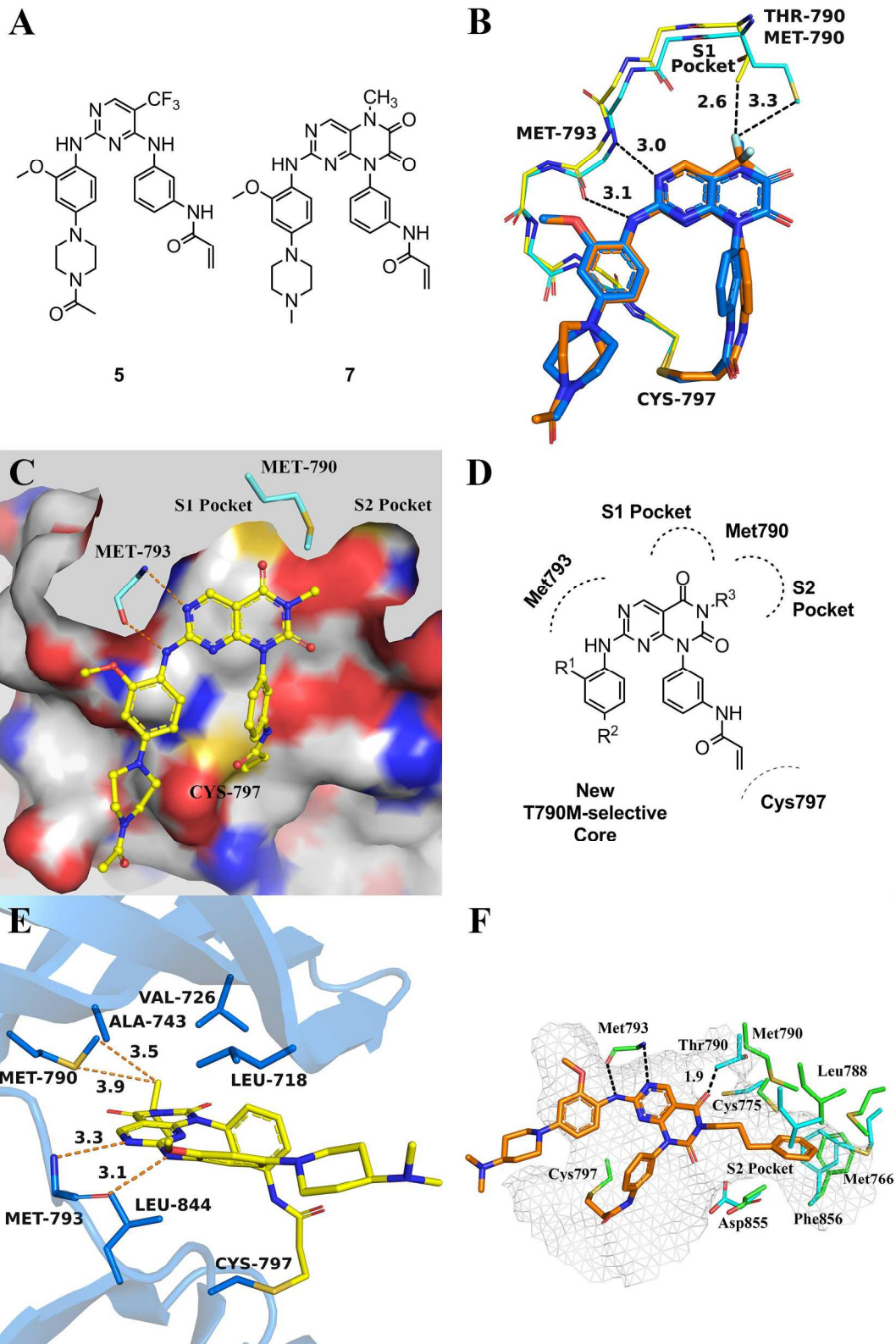


Figure 3

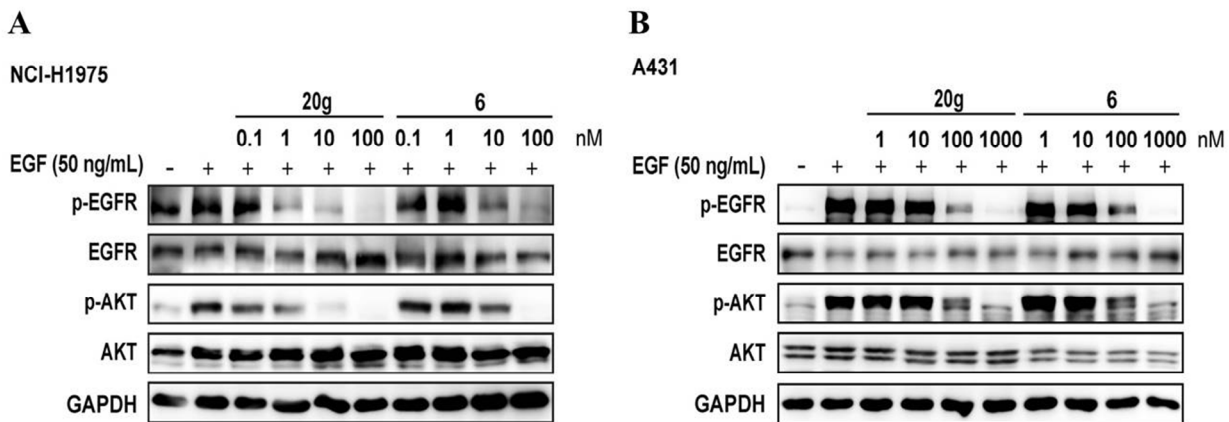


Figure 4

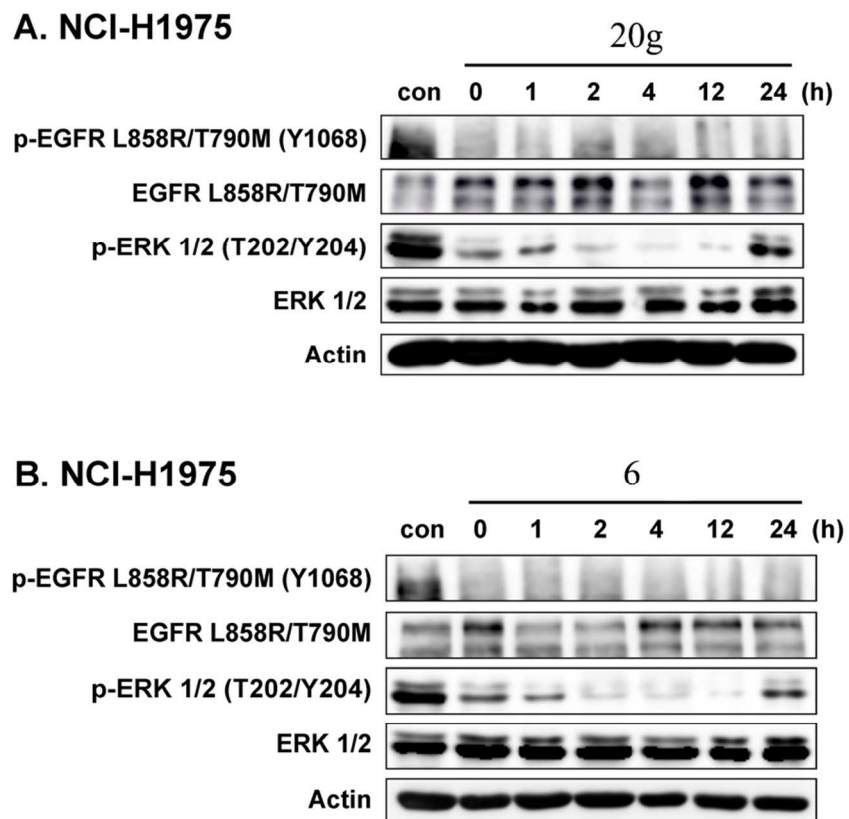
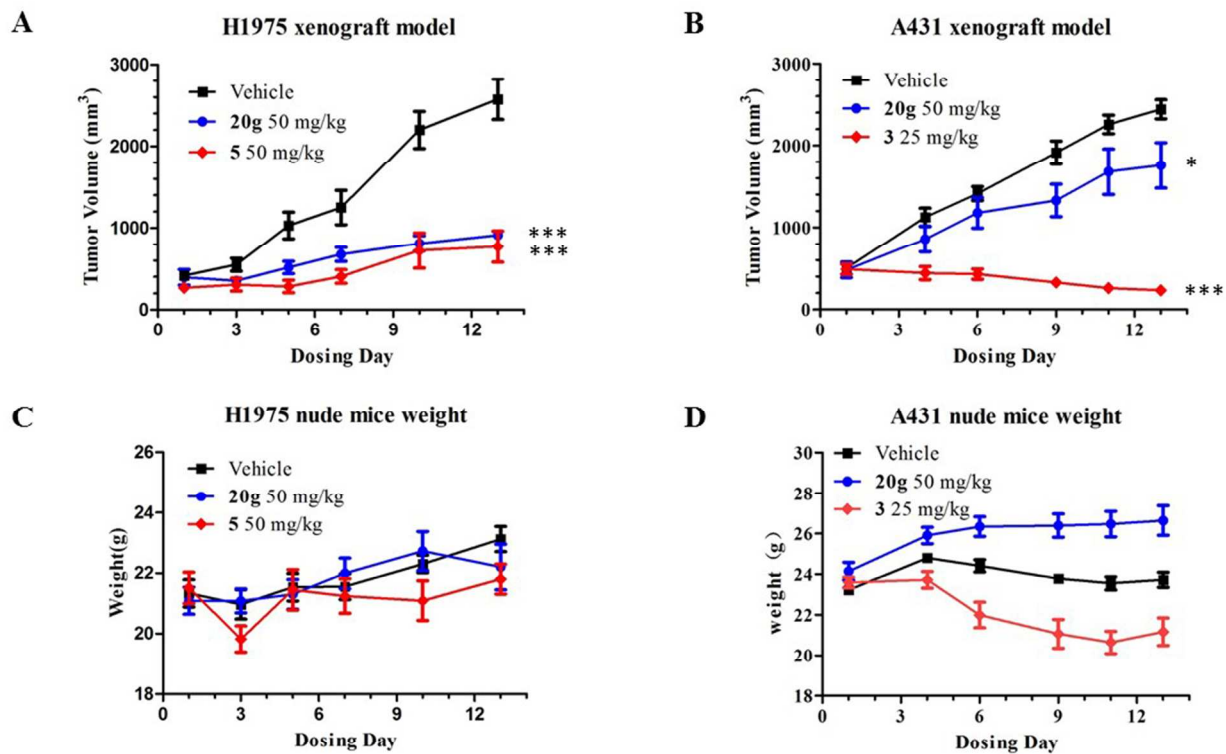
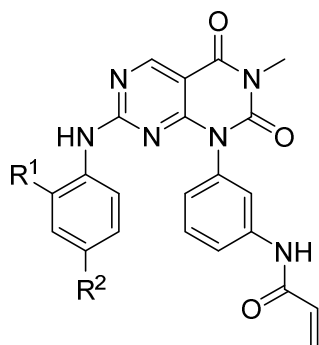


Figure 5



TABLES

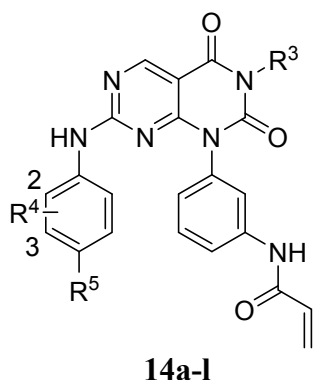
Table 1. In Vitro EGFR Inhibitory Activity and Antiproliferation Activity of Compounds

14a-e^a

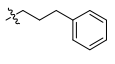
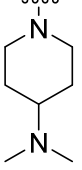
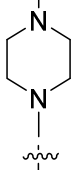
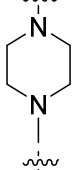
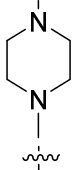
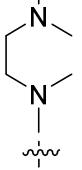
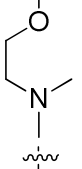
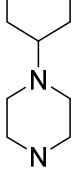
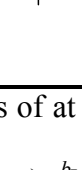
Compd.	R ¹	R ²	Enzyme inhibitory activity (IC ₅₀ , nM)		Enzyme Selectivity WT:DM	Cellular antiproliferative activity (IC ₅₀ , nM)		Cellular Selectivity A431: H1975	Solubility (μg/mL) @PBS (pH 7.4) ^c
			WT	L858R/ T790M		A431	H1975		
14a	-OCH ₃		180±79	46±26	3.9	> 10000	> 10000	ND ^b	< 10
14b	-OCH ₃		341±341	70±34	4.9	> 10000	> 10000	ND	61
14c	-OCH ₃		314±113	91±12	3.5	8373±1970	573±144	15	45
14d	-OCH ₃		137±2.8	30±6.9	4.6	3892±3642	230±142	17	531
14e	H	H	82±63	68±39	1.2	> 10000	9264±4791	ND	< 10
5			272±127	20±2.9	14	641±282	31±34	21	

^aKinase activity assays were examined by using the ELISA-based EGFR-TK assay. The antiproliferation activity of the compounds were employed by using the sulforhodamine B (SRB)

1
2
3 colourimetric assay. Data are averages of at least three independent determinations and reported
4
5 as the means \pm SDs (standard deviations). ^bNot determined. ^cAqueous solubility of these
6
7 derivatives was examined by using UV-visible spectrophotometer in PBS buffer (0.1 M, pH 7.4).
8
9
10
11
12
13
14
15
16
17
18
19
20
21
22
23
24
25
26
27
28
29
30
31
32
33
34
35
36
37
38
39
40
41
42
43
44
45
46
47
48
49
50
51
52
53
54
55
56
57
58
59
60

Table 2. In Vitro EGFR Inhibitory Activity and Antiproliferation Activity of Compounds**20a-l^a**

Compd.	R ³	R ⁴	R ⁵	EGFR enzyme inhibitory activity (IC ₅₀ , nM)		Enzyme Selectivity WT:DM	Cellular antiproliferative activity (IC ₅₀ , nM)		Cellular Selectivity A431: H1975	Solubility (μg/mL) @PBS (pH 7.4) ^c
				WT	L858R/ T790M		A431	H1975		
20a		2-OCH ₃		111±31	2.5±0.2	44	> 10000	175±122	ND ^b	229
20b		2-OCH ₃		13±1.6	0.4±0.3	33	4130±2559	60±34	69	184
20c		2-OCH ₃		20±14	0.8±0.3	25	> 10000	50±27	ND	176
20d		2-OCH ₃		1.2±0.3	1.9±0.2	0.6	3300±909	278±166	12	137
20e		2-OCH ₃		0.7±0.4	1.0±0.2	0.7	2043±963	189±150	11	99

1											
2											
3											
4											
5	20f		2-OCH ₃		3.8±1.3	1.4±0.4	2.7	1463±271	358±185	4.1	104
6											
7											
8											
9											
10											
11	20g		2-OCH ₃		79±14	0.3±0.2	263	1564±763	44±48	36	262
12											
13											
14											
15											
16	20h		3-OCH ₃		119±22	6.8±2.8	18	1047±370	37±28	28	309
17											
18											
19											
20											
21	20i		3-CH ₃		34±16	1.0±0.9	34	954±450	24±20	40	280
22											
23											
24											
25											
26	20j		2-OCH ₃		121±18	16±5.7	7.6	1949±1260	138±79	14	1054
27											
28											
29											
30											
31	20k		2-OCH ₃		227±93	115±13	2.0	3600±3685	99±54	36	647
32											
33											
34											
35											
36											
37											
38	20l		2-OCH ₃		240±67	14±7.6	17	1385±123	154±141	9.0	121
39											
40											
41											
42											
43											
44	5				272±127	20±2.9	14	641±282	31±34	21	
45											

^aData are averages of at least three independent determinations and reported as the means ± SDs (standard deviations). ^bNot determined. ^cAqueous solubility of these derivatives was examined by using UV-visible spectrophotometer in PBS buffer (0.1 M, pH 7.4).

Table 3. Mouse Pharmacokinetics Parameters for Compound 20g

Dose (route)	$T_{1/2}$ (h)	T_{max} (h)	C_{max} (ng/mL)	$AUC_{(0-t)}$ (ng·h/mL)	$AUC_{(0-\infty)}$ (ng·h/mL)	V_z (mL/kg)	CL (mL/h/kg)	F (%)
1 mg/kg (IV)	0.9	0.1	311	181	186	4530	5370	-
10 mg/kg (PO)	1.1	2.0	271	650	658	-	-	35

Table of Contents Graphic

